

Fabrication of intermediate temperature fuel cell based on ceria-based electrolyte

A Dissertation submitted in fulfillment of the requirements for the Degree
of

MASTER OF SCIENCE

in

PHYSICS

Submitted by

Raman Kumar

Roll No. 301704026

Under the Guidance of

Dr Jayant Kolte

Asst. Professor, SPMS



THAPAR INSTITUTE
OF ENGINEERING & TECHNOLOGY
(Deemed to be University)

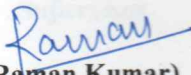
2019

School of Physics and Material Science
Thapar Institute of Engineering & Technology, Patiala
(Declared as Deemed-to-be-University u/s 3 of the UGC Act., 1956)
Post Bag No. 32, Patiala – 147004
Punjab (India)

DECLARATION

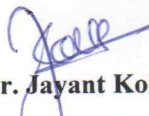
I hereby certify that the work which is presented in dissertation entitled, "**Fabrication of intermediate temperature fuel cell based on ceria-based electrolyte**" in partial fulfilment of the requirements for the award of the degree of Masters In Physics, School of Physics and Material Science, Department of Thapar Institute of Engineering & Technology (Deemed to be University) is as authentic record of my own work carried under the supervision of Dr. Jayant Kolte. It refers others researcher's work which are duly listed in the reference section. The matter contained in this dissertation has not been submitted, neither in part nor in full to any other degree to any other university or institute except as reported in text and references.

Place: Patiala, Punjab
Date: 29/08/2019


(Raman Kumar)
Roll No.: 301704026

It is certified that the above statement made by the student is correct to the best of my knowledge and belief.

Date: 29/8/19


(Dr. Jayant Kolte)
Assistant Professor

School of Physics and Material Science,
Thapar Institute of Engineering & Technology, Patiala

CERTIFICATE


Certified that the dissertation entitled, "Fabrication of intermediate temperature fuel cell based on ceria-based electrolyte", which is being submitted by Raman Kumar in fulfillment of the requirements for the award of the M.Sc. Physics, to Thapar Institute of Engineering & Technology (Deemed to be University), is a bonafide record of the candidate's own work carried out by him under my supervision and guidance. The matter contained in this dissertation has not been submitted, neither in part nor in full to any other university or institute for award of any degree.

Place:

Patiala, Punjab

Date:

29/8/19


(Dr. Jayant Kolte)
Supervisor

ACKNOWLEDGMENT

First of all, I would like to thank to the Almighty, who is the creator of this universe without his will even the single leaf doesn't have the competence to move, it is his mercy and blessing to me that this work become possible.

I would like to express my sincere gratitude to my supervisor Dr. Jayant Kolte for his unlimited guidance, insight and suggestions throughout the research. I thank him from the bottom of my heart for introducing me to the area of electro ceramics. I thank him for his great patience, constructive criticism and myriad useful suggestions apart from invaluable guidance to me.

I am grateful to Dr O.P. Panday, Head of School of Physics and Material Science (SPMS) for his encouragement and help to carry out the thesis work.

I am also indebted to my senior research colleague Mr Savidh Khan for his unconditional support and constant motivation whenever needed.

I am very grateful to my dear friend Mr Qaiser Yousuf who have given me his friendship, put up with my odd hours, and provided me with lifts and practical help.

Last but not the least, I would like to thank my dear parents, my elder brother, my beloved sisters for their support, without their support it was not possible to come so far.

RAMAN KUMAR

(301704026)

ABSTRACT

Ceria based electrolyte are most suitable electrolyte for Intermediate temperature Solid Oxide fuel cell. In this present work gadolinium doped ceria ($\text{Gd}_{0.1}\text{Ce}_{0.9}\text{O}_2$) was prepared via sol-gel process. FTIR analysis shows that at calcination temperature of 600°C most of the organic materials are removed from the samples. The prepared and calcined powder was characterized with XRD, FTIR, SEM, TGA/DTA, I-V and impedance analysis. Single phase cubic fluorite structure is confirmed by XRD analysis where as highly dense microstructure of the pellet sintered 1450°C was confirmed by SEM analysis with a 98% relative density. High temperature sintering results in a significantly high ionic conductivity of $3.04 \times 10^{-1}\text{ S/cm}$ at 600°C in air atmosphere for pellet sintered at 1450°C . Complex impedance spectra with well defined, regular and symmetrical semi-circles, was observed in accordance to bricklayer theoretical model. From impedance spectroscopy analysis, it is clear that the two semi-circles start merging together and thus bulk and grain boundary conductivity can not be completely distinguished and grain boundary arc also start disappearing.

TABLE OF CONTENTS

Certificates.....	i
Acknowledgement.....	ii
Declaration.....	iii
Abstract.....	iv
Table of contents.....	v
List of figures.....	vii
CHAPTER-1 INTRODUCTION.....	1
1.1 Energy	1
1.2 Energy classification and energy crises	1
1.3 Solid oxide fuel cell (sofc)	3
1.4 Why gadolinium doped ceria (gdc)?	4
1.5 References.....	6
CHAPTER-2 LITERATURE REVIEW	8
2.1 References.....	15
CHAPTER-3 EXPERIMENTAL DETAILS	18
3.1 Synthesis of GDC (electrolyte) material	18
3.2 Binder Solution Preparation	20
3.3 Pellet formation	21
3.4 Phase analysis.....	22
3.5 Microstructural analysis	22
3.6 Impedance analysis	23
3.7 TGA (Thermogravimetry Analysis).....	24
3.8 Fuel Cell test.....	24
CHAPTER-4 RESULTS AND DISCUSSION	26
4.1 Structural analysis	27
4.2 FTIR analysis	28
4.3 Surface Morphology.....	30
4.4 Thermal Analysis	31
4.5 Leakage current study	32
4.6 Conductivity Measurement	35

4.7	Temperature and frequency dependent conductivity	37
4.8	Cell test.....	37
4.9	References	
SUMMARY AND FUTURE SCOPE.....		40

LIST OF FIGURES

FIG 1.1	Worldwide energy generation from different sources of energy from renewable and non-renewable energy sources	1
FIG 1.2	The energy by the various sources, estimated from 1965-2095	2
FIG 1.3	Fig 1.3 (a)Cubic fluorite structure of ceria, and (b) oxygen vacancy in acceptor doped ceria system	4
FIG 1.4	Conductivity of various electrolyte	5
FIG 3.1	Flowchart of the synthesis process of Ce _{0.9} Gd _{0.1} O _{1.95} via sol gel process	19
FIG 3.2	Flow chart for the plan of work	20
FIG 3.3	X'PERT MRD powder X-Ray Diffractometer	22
FIG 3.4	Scanning Electron Microscope used to study the surface morphology of GDC	23
FIG 3.5	Impedance analyser used for dielectric measurement	23
FIG 3.6	Thermogravimetry Analyser	24
FIG 3.7	(a) shows the schematic assembly of Probostat TM component for fuel cell measurement and (b) shows the schematic assembly of Probostat TM base unit	25
FIG 4.1	XRD pattern of as prepared sample & GDC powders calcined at 200, 400, 600 °C for 2hrs in air	26
FIG 4.2	FTIR spectra of as-prepared GDC powders and calcined powder at 200, 400, 600°C	27
FIG 4.3	(a) SEM micrograph of surface of GDC samples calcined at 600 1C for 2h (5000x) and GDC sample sintered at (b) 1250 °C, (c) 1350 °C and 1450°C for 6 h (10000x)	27
FIG 4.4	TGA and DTA thermograph of as prepared GDC powder	29
FIG 4.5	I-V characteristics of GDC pellets sintered at 1250, 1350,1450 °C	30
FIG 4.6	Cole-Cole plot of GDC pellet sintered at 1250° C in temperature range from 150-600° C. The fitted data is represented by solid line	31
FIG 4.7	Cole-Cole plot of GDC pellet sintered at 1350° C in temperature range from 150-600° C. The fitted data is represented by solid line	32

FIG 4.8	Cole-Cole plot of GDC pellet sintered at 1450° C in temperature range from 150-600° C. The fitted data is represented by solid line	32
FIG 4.9	Grain conductivity as a function of temperature for all the sample sintered at different temperature	33
FIG 4.10	(a), (b), (c) AC conductivity behaviour with frequency of sintered sample in temperature range 200-500° C, (d) Variation of $\ln(\sigma)$ with $1000/T$ to find out the activation energy of the samples	35
FIG 4.11	Power density measuremet of the GDC sample sintered at 1450° C	39

1.1 Energy

Energy, in simple word can be define as the ability of a physical system to do work. Various from of energy exist in nature which includes potential, thermal, kinetic, nuclear etc. For simple illustration energy is something that help in achieving motion by pushing or pulling the things around. Most commonly, energy is measured in joules, but instead of joules other units of energy are includes BTUs, newton or may be in calories [15]. In this context, we are dealing with electrical energy. Unit of electrical energy is kilo watt-hour.

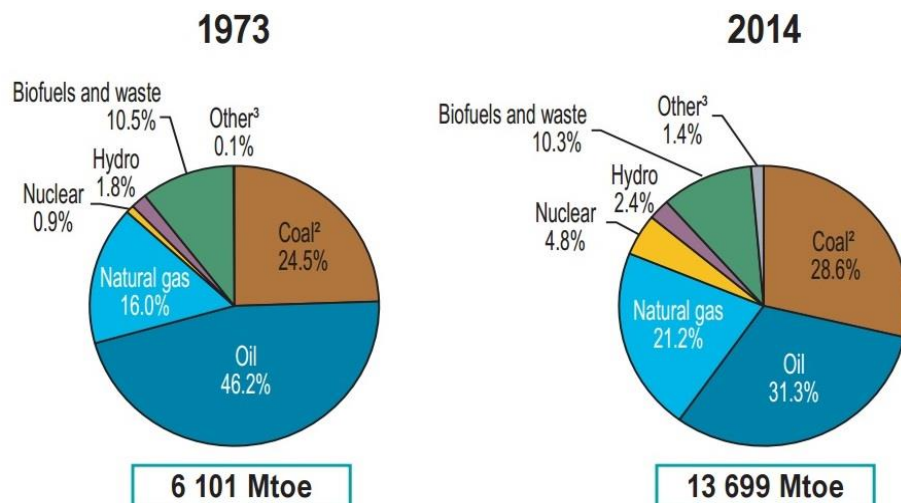


Fig 1.1 Worldwide energy generation from different sources of energy from renewable and non-renewable energy sources [15]

1.2 Energy Classification and Energy Crises

Energy sources may be classified as (a) renewable sources of energy (b) non-renewable sources of energy. Fig 1.1 shows the worldwide energy generation from different sources of renewable and non-renewable energy sources. Energy sources that can be reused again are known as renewable sources of energy e.g. solar energy, wind energy, hydroelectric energy, geothermal energy, biomass energy, ocean energy, hydrogen energy and the energy sources that cannot be form or replenish in a short period of time are known as non-renewable sources of energy e.g. crude oil, natural gas, coal, uranium.

Since we are familiar with the fact that the natural sources of energy are limited in supply and the world's demand on these limited sources of energy is increasing day by day. This may lead to energy crisis as these sources take thousands of years to replenish once they get finished. The main reason for energy crises is overconsumption, overpopulation, poor infrastructure, poor distribution system, wastage of energy, unexplored renewable energy options etc. one of the most possible solution of the energy crises is to shift toward the renewable sources of energy.

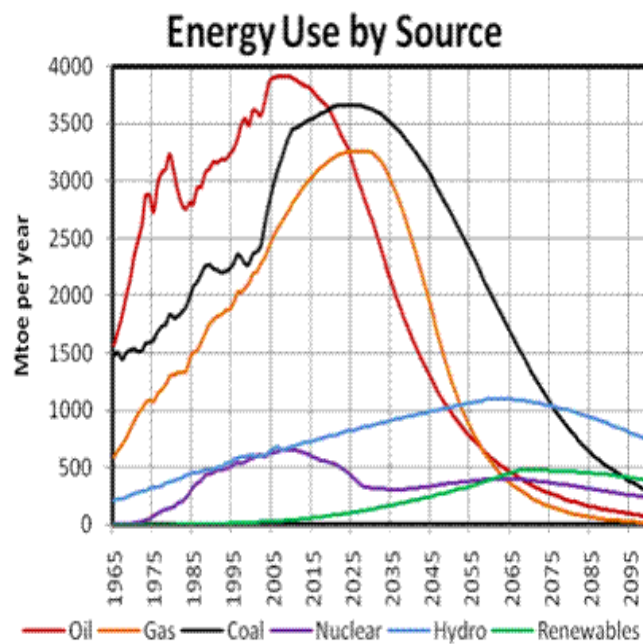


Fig 1.2 The energy by the various sources, estimated from 1965-2095[16]

From Fig 1.2 is can we clearly seen that up to year 2095 most of the share of energy production will come from the renewable sources of energy. Various renewable sources can be used for energy production like wind energy, solar energy etc. likewise a fuel cell can also be attributed as an efficient way of energy production. Fuel cell technology offers clean, reliable and efficient power generation. There are many types of fuel cells available viz. Solid Oxide Fuel cell (SOFC), Proton-exchange membrane fuel cell (PEMFC), Direct methanol (DMFC), Alkaline fuel cell (AFC), Phosphoric acid fuel cell (PAFC), Molten carbonate fuel cell (MCFC), Regenerative Fuel cell (RFC), Zinc air fuel cell (ZAFC), Microbial fuel cell (MFC) etc. Our main focus in this discussion will be on SOFC i.e. Solid oxide Fuel Cell.

1.3 Solid Oxide Fuel Cell (SOFC)

Solid oxide fuel cell (SOFC) is an energy conversion device with an efficiency ~ 40-70% with regeneration [1]. It is a renewable, clean, versatile source of energy that convert the chemical energy into electrical energy [2,3]. The electrolyte used in this type of fuel cell is solid electrolyte like ceramics that is why it gets the name solid oxide fuel cell. Every basic fuel cell has three components viz. an anode, cathode and an electrolyte. Based upon the operating temperature the SOFCs are classified into three categories i.e. HT (High Temperature)-SOFCs, IT (Intermediate Temperature) -SOFCs, and LT (Low Temperature)- SOFCs. The operating temperature range of HT-SOFCs, IT-SOFCs and LT-SOFCs is 800-1000 °C, 500-800 °C and below 500 °C respectively.

HT-SOFC requires very high operating temperature which reduces its application on commercial basis and also increase the fabrication cost [4]. As reported, the most suitable electrolyte material for HT-SOFCs is Yttria Stabilized Zirconia YSZ which require an operating temperature range of ~800-1000 °C. However thermal mismatch between materials, interfacial reaction electrode/electrolyte materials and electrode/interconnect interface are some of the destructive factor of high temperature [5] and hence there is requirement for an effective replacement with some other electrolyte materials. The ceria-based electrolyte material which have high ionic conductivity of order 10^{-2} S/cm at intermediate temperature range (500-800 °C) can be helpful to overcome all these problems that is why it has received a great attention in the recent years [6].

This study is based on the fabrication and testing of the electrolyte material for IT-SOFCs. GDC (Gadolinium Doped Ceria) is reported as one of the most suitable electrolyte materials for IT-SOFC [7-11] due to the following attributes (a) prevention from mixing the electrode gases via forming a link between anode and cathode [12], (b) Stable chemical structure in oxidising as well as reducing atmosphere [13,14], (c) optimal physical properties (thermal expansion 100-873 K, mechanical strength etc), (d) minimum ohmic loss, (e) easy densification upon sintering etc. CeO₂-based material have fluorite structure (Fig 1.3) & possess face centred cubic arrangement of cation and the anion occupying the tetrahedral voids. The pure CeO₂ do not have sufficient oxygen ions vacancy for achieve a high ionic conductivity, hence in order to achieve high ionic conductivity, oxygen ion vacancy is introduced into the structure via replacement of host Ce⁴⁺ by acceptor cations, such as, Gd³⁺, Sm³⁺, or Y³⁺.

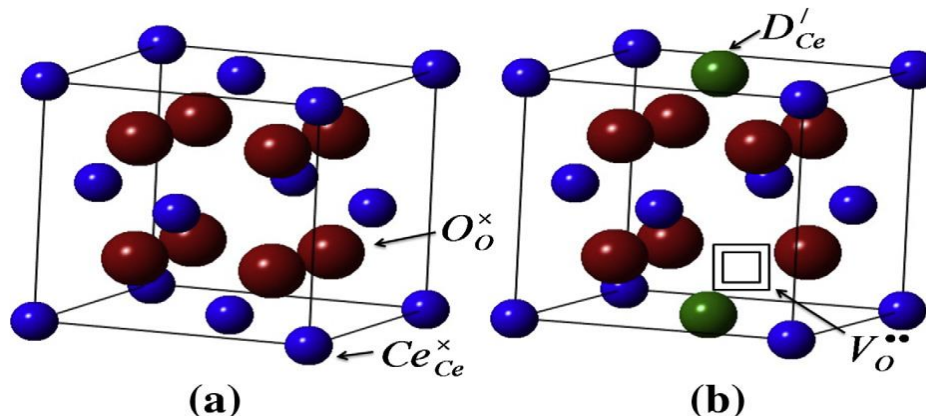


Fig 1.3 (a)Cubic fluorite structure of ceria, and (b) oxygen vacancy in acceptor doped ceria system [1]

The GDC powder is prepared by adding 10mol% Gd in CeO_2 via sol-gel method, followed by various characterization viz. x-ray diffraction, scanning electron microscope, thermal gravimetric analysis, Fourier transformation IR analysis, Impedance analysis, IV characteristic, Cell testing (Power measurement). The series of the sample contains the powder without calcination (as-prepared), that calcined at 200 °C, 400 °C and 600°C (200GDC, 400GDC, 600GDC respectively) and sintered pellets at 1250 °C, 1350 °C and 1450 °C (1250GDC, 1350GDC, 1450GDC respectively) for 6hrs.

1.4 Why gadolinium doped ceria (GDC)?

For intermediate temperature dopant like Gd^{3+} , Sm^{3+} , or Y^{3+} can be used but Gd^{3+} dopant is reported as one of the best dopants for IT-SOFCs because:

- very high ionic conductivity ($8.38 \times 10^{-2} \text{ S cm}^{-1}$) at 600 °C
- Chemically and structurally stable.
- A sufficient dense GDC membrane can be easily created to avoid gas leakage across both the electrodes

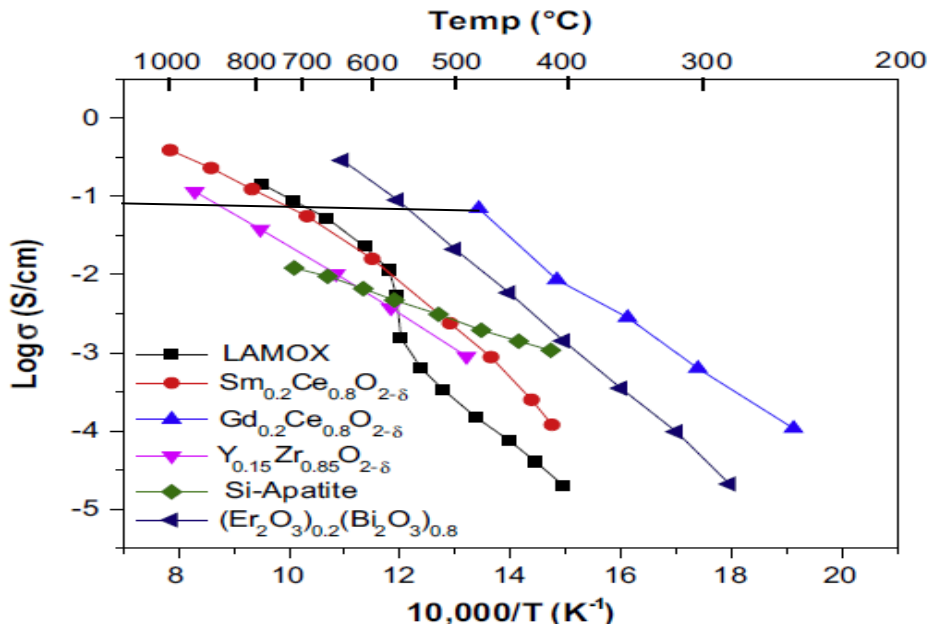


Fig 1.4 Conductivity of various electrolyte [1]

Fig 1.4 show the conductivity of various electrolyte for various electrolyte used for solid oxide fuel cell. For IT-SOFCs among the dopants Gd³⁺, Sm³⁺, or Y³⁺. It is clearly seen from Fig 1.4 that Gd has very high ionic conductivity at a relative low temperature than the other two dopants. Hence Gd is the most suitable electrolyte material for the intermediate temperature fuel cell applications

REFERENCES

1. Neelima Mahato, Amitava Banerjee, Alka Gupta, Shobit Omar, Kantesh Balani, Progress in material selection for solid oxide fuel cell technology: A review, *Progress in Materials Science* 72, 2015, 141–337J.
2. James E. Mason, World energy analysis: H₂ now or later? *Energy Policy* 35, 2007, 1315–1329.
3. Chris Greena, Soham Baksib, Maryam Dilmaghani, Challenges to a climate stabilizing energy future, *Energy Policy* 35, 2007, 616–626
4. J. Will, A. Mitterdorfer, C. Kleinlogel, D. Perednis, L.J. Gauckler, Fabrication of thin electrolytes for second-generation solid oxide fuel cells, *Solid State Ionics* 131, 2000, 79–96.
5. Aliye Arabacıa, M.Faruk Oksuzomer, Preparation and characterization of 10mol% Gd doped CeO₂ (GDC) electrolyte for SOFC application, *Ceramics International*, 2012,38, 6509-6515.
6. H. Inaba, H. Tagawa, Ceria-based solid electrolytes, *Solid State Ionics*, 83, 1996, 1–16.
7. V. Esposito, E. Traversa, Design of electroceramics for solid oxide fuel cells applications: playing with ceria, *Journal of the American Ceramic Society* 91 2008, 1037–1051.
8. J. Cheng, S.Zha, X.Fang,X.Lin,G.Meng,On the green density, sintering behaviour and electrical property of tapecast Ce_{0.9}Gd_{0.1}O_{1.95} electrolyte films, *Materials Research Bulletin*,37, 2002, 2437–2446.
9. B.C.H.Steele, Appraisal of Ce_{1-y}Gd_yO_{2-y/2} electrolytes for IT-SOFC operation at 500 1C, *Solid State Ionics*, 129, 2000, 95–110.
10. C.Xia, M.Liu, Low-temperature SOFCs based on Ce_{0.9}Gd_{0.1}O_{1.95} fabricated by dry pressing, *Solid State Ionics*, 144, 2001, 249–255.
11. R.O.Fuentes,R.T.Baker, Structural, morphological, and electrical properties of Ce_{0.9}Gd_{0.1}O_{1.95} prepared by a citrate complexation method, *Journal of Power Sources*,186, 2009, 268–277.
12. K.R. Reddy, K. Karan, Sinterability, mechanical, microstructural, and electrical properties of gadolinium-doped ceria electrolyte for low-temperature solid oxide fuel cells, *Journal of Electro ceramics*, 15, 2005, 45–56.

13. V.V. Kharton, F.M.B. Marques, Mixed ionic-electronic conductors: effects of ceramic microstructure on transport properties, *Current Opinion in Solid State and Materials Science*, 6, 2002, 261–269.
14. R.M. Ormerod, *Solid oxide fuel cells*, The Royal Society of Chemistry, 32, 2003, 17–28.
15. <https://interestingengineering.com/all-of-the-energy-generation-systems-in-the-world> (copied)
16. <http://321energy.com/editorials/deruijter/deruijter021109.html?print=on>

CHAPTER 2

LITERATURE REVIEW

1. Arabacia-et-al have studied that ceria-based materials are best suitable materials for intermediate temperature solid oxide fuel cell as well as and low temperature solid oxide fuel cell. GDC with composition ($Gd_{0.1}Ce_{0.9}O_{1.95}$) was prepared by doping 10% Gd in fully dense CeO_2 ceramics by Pechini method. Fluorite structure with single phase was found at calcination temperature of $500^\circ C$ for 1 hr. Analysis of the material if followed by various characterization techniques like X ray diffraction, differential thermal analysis (DTA), High temperature FTIR and thermal-gravimetric analysis (TGA). Pellet density with 98% was observed at sintering temperature 1400 for 6 hrs. At $500^\circ C$, total ionic conductivity of $3.4 \times 10^{-2} S cm^{-1}$ was achieved. Thus, Pechini method is more favourable low temperature technique to obtain, good total ionic conductivity and high density of $Gd_{0.1}Ce_{0.9}O_{1.95}$ powder. [1]
2. K.C. Anjaneya-et-al have reported the preparation gadolinium doped ceria (GDC) for intermediate temperature solid oxide fuel cell with composition $Ce_{0.8}Gd_{0.2}O_2$ by EDTA-citrate complexing method electrolyte at different ph. Characterization analysis includes TEM, FE-SEM, Raman, Electrochemical impedance spectroscopy. Cubic fluorite structure with space group Fm3m was analysed by the XRD pattern of GDC powder calcined at 873 K for 5 hrs. Formation of the solid solution of sintered GDC powder was confirmed by Raman. Well defined grain separated from grain boundaries with good densification of the sintered GDC pellets at different pH was analysed by FE-SEM and hence obtain the relative density of 99% and maximum conductivity $1.6 \times 10^{-2} S cm^{-1}$ at 973 K for GDC pellet with pH = 10 which make GDC a potential electrolyte.[2]
3. A.Zarkova-et-al have employ the sol-gel synthesis and sol-gel combustion route synthesis for preparation of GDC electrolyte material for intermediate temperature solid oxide fuel cell. Both procedures use the same complexing agents for preparation of 10% GDC powder ($Gd_{0.1}Ce_{0.9}O_{1.95}$). TGA and DSC analyse the thermal behaviour of the powder. The crystallinity and purity of the phase was governed by X-ray spectroscopy techniques. Estimation of surface morphological feature was done by Scanning electron microscopy (SEM). For the analysis of specific surface area nitrogen adsorption–desorption and for the surface composition X-ray photoelectron spectroscopy (XPS)

was employed. Impedance spectroscopy measure the electrical properties of the synthesised sample.[3]

4. J. Yang-et-al prepare the fluorite oxides $\text{Ce}_{0.8}\text{Y}_{0.18}\text{M}_{0.02}\text{O}_{2-\delta}$ (denoted as MYDC for M = Sr, La, Fe and Ca) by the sol-gel method which is used as electrolytes for IT-SOFCs. Single phase cubic fluorite structure which is highly pure of all the composition was obtained which was analysed by X ray spectroscopy technique. Scanning electron microscope (SEM) analyse the surface morphology and measures the relative density which is more than 95 % of all sample sintered at temperature 1400°C . In the temperature range from 400 to 800°C , the ionic conductivity was studied by AC impedance spectroscopy and from this data it was found that the conductivity of 0.057 S cm^{-1} was shown by $\text{Ce}_{0.8}\text{Y}_{0.18}\text{La}_{0.02}\text{O}_{2-\delta}$ which found the good application in intermediate temperature solid oxide fuel cell (IT-SOFCs).[4]
5. S.M. Jamil-et-al have studies how much effectiveness does the nano size GDC particle will show to get the dense GDC electrolyte at low sintering temperature. Fabrication of the SOFCs will be greatly benefitted by lowering the sintering temperature. A doped suspension with 30% nano sized loading was prepared and then casted into flat sheet with the help of phase inversion technique. This sheet undergoes mechanical strength, morphology and surface roughness test. With the help of Phase inversion-based co-extrusion/co-sintering technique, electrolyte/anode dual-layer hollow fibres (DLHFs) half-cell of MT SOFCs were fabricated followed by morphological and gas fitness test. The result depicted that 30% nanoparticle sintered at temperature at 1450°C , lower than those reported by 50°C at 100%-micron particle leads to formation of dense and gas tight layer CGO layer. Maximum power density comes out to be 0.66 W cm^{-2} with H_2 as fuel. This is a recommended technique for the manufacturing of low- cost- dual layer hollow microtubular SOFCs.[5]
6. G.Accardo-et-al have synthesises the Gadolinium doped ceria with composition $(\text{Gd}_{0.1}\text{Ce}_{0.9}\text{O}_{1.95})$ by urea-based co-precipitation method (UBHP). At 400°C calcination temperature a single fluorite structure was observed. The obtained powder along with the agglomerations have grain in nanometric size but have overall good sinterability. The sintered pellet at 1300 and 1500°C . The relative density of 95% and a uniform microstructure of grains in few microns was observed for the pellet sintered at 1500°C for 3hrs. the conductivity of a sample is remarkably good in range from $1.1 \times 10^{-2}\text{ S cm}^{-1}$ to $4.1 \times 10^{-2}\text{ S cm}^{-1}$ in temperature range of 650 to 800°C . These promising

conductivity values of the synthesised powder make GDC a prominent material for the application on IT- SOFCs.[6]

7. E.H.Hyeong-et-al have synthesise highly sinterable nanocrystalline cerium oxide-based materials like Gd_2O_3 doped and Sm_2O_3 doped CeO_2 electrolytes using the sonochemical method. X ray spectroscopy analyse the crystallinity and the grain size whereas size of the nanocrystal in range 5 to 7 nanometres was confirmed by transmission electron microscope (TEM). Using this sonochemical technique the sintering temperature was reduced to $200^\circ C$ than the conventional sintering temperature i.e. $1550^\circ C$. Microstructural and sintering characterization confirm this significant improvement in this reduce sintering temperature.[7]
8. Chandradass-et-al have prepare the gadolinium doped ceria (GDC) nanoparticle for which oil phase is taken as cyclohexane, Igepal CO 520 as non-ionic surfactant and the aqueous solution of $(Gd(NO_3)_3 \cdot 6H_2O)$ and $(Ce(NO_3)_3 \cdot 6H_2O)$ as the water phase in reverse micromulsion system. With the variation in the surfactant to water molar ratio the particle size is controlled. Characterization the prepared and calcined GDC powder includes thermo gravimetry analysis (TGA) and differential thermal analysis (DTA), scanning electron microscopy (SEM), Raman Spectroscopy, energy dispersive spectroscopy (EDS), transmission electron microscopy (TEM), Fourier transform infrared spectroscopy (FTIR) and X-ray diffraction spectroscopy (XRD). The single-phase cubic fluorite was observed at $700^\circ C$ calcination temperature which is verified by the XRD results. As there appear an increment in water to surfactant molar ratio (R) the average size of the particle was found to be increase. SEM reveals that the particle's diameter for various R varies between 8-15 nm and for TEM it is between 7.5-11 nm. Presence of gadolinium and ceria phase was confirmed by EDS analysis at $700^\circ C$ calcination temperature. At room temperature formation of solid solution of GDC was confirmed by Raman spectroscopy and FTIR confirms the elimination of residual oil and surfactant phase from the microemulsion-derived precursor and calcined powder.[8]
9. H.P.Dasari-et-al provides a more efficient way to significantly reduce the sintering temperature as high temperature ($> 1300^\circ C$) requirement for sintering is one of the major problems with Solid Oxide Fuel Cell to make the electrolyte material fully dense. GDC nano crystal was prepared by co-precipitation method and the full density results from the combine effect of microwave sintering and liquid-phase sintering mechanism, and particle size reduction. In liquid phase sintering lithium (Li) is used as an additional

dopant. The electrolyte material results from microwave sintering show a significant decrease in the sintering temperature to 600° C. As compared to GDC sample, the implication of Li addition can be clearly seen from Scanning Electron Microscopy (SEM), transmission Electron Microscopy (TEM) micrograph that brightly shows huge growth in grain-size of Li-GDC sample (~150 nm) with high ionic conductivity and activation energy of $1.00 \times 10^{-2} \text{ S cm}^{-1}$ and 0.53 eV respectively for Li-GDC at 600 °C in air.[9]

10. L.Khan-et-al have studied the enhanced stability and mechanical strength of composite electrolyte of lithium sodium carbonate and GDC synthesised via melt infiltration technique for application as SOFC electrolytes. At 1450° C sintering temperature porous matrix of GDC is synthesis and then mixture of lithium sodium carbonate is melt infiltrated with (1:1 wt. ratio). I-V characteristics, Ionic conductivities and impedance spectra with hydrogen as fuel in air of supported bilayers are measured. X-ray diffraction, Fourier transform infrared spectroscopy, energy dispersive spectroscopy (EDS), scanning electron microscope (SEM) are done for the physical characterization of electrolyte. Thermal gravimetric analysis (TGA) show that the GDC matrix is completely filled by carbonate phase. Melt infiltrated 30 wt.% lithium carbonate and GDC composite electrolyte ionic conductivity is comparable to the electrolyte synthesised by solid state reaction method at 600° C and its performance is much better (223 mW cm^{-2} at 579 mA cm^{-2}) than electrolyte material synthesised solid state reaction at temperature of 750°C. The TGA, morphological and electrochemical studies show a better cell performance which is due to better sintered stable structure.[10]
11. H.Okaya-et-al had employ ultrasound assisted co-precipitation method to synthesis $\text{Ce}_{1-x}\text{Gd}_x\text{O}_{2-x/2}$ and $\text{Ce}_{1-x}\text{Nd}_x\text{O}_{2-x/2}$ ($x = 0.05, 0.10, 0.15, 0.20$ and 0.25). With dopant concentration, the ionic conductivity using impedance spectroscopy was studied over 300–800°C temperatures in air. The maximum total ionic conductivity of 4.01×10^{-2} and $3.80 \times 10^{-2} \text{ S cm}^{-1}$ with activation energy of $0.828 \text{ kJ mol}^{-1}$ and $0.838 \text{ kJ mol}^{-1}$ at 800° C temperature was observed for $\text{Ce}_{0.90}\text{Gd}_{0.10}\text{O}_{1.95}$ and $\text{Ce}_{0.85}\text{Nd}_{0.15}\text{O}_{1.925}$ electrolyte respectively. The grain size is in the range of 0.3-0.6 microns and 0.2-0.4 microns for GDC and NDC respectively. Using the ultrasound assisted co-precipitation method a uniform fine crystallite size powder can be prepared leading to highly dense sintered pellet at 1200° C for 5 hrs. [11]
12. C.Son-et-al have employed the solid-state reaction route to synthesis 10mol% gadolinium doped cerium (IV) oxide. The prepared sample, with the help of thermal

(plasma) spray techniques deposited as thick film. Scanning electron microscopy (SEM), x ray spectroscopy (XRD) and atomic force microscopy (AFM) are used for phase development, microstructure and topography analysis of the prepared sample. Pull off adhesion test measure the mechanical strength of the deposited film. A DC four probe conductivity experiment was performed to measure the electrical properties of plasma-sprayed GDC and the maximum conductivity was found to be $3.60 \times 10^{-2} \text{ S cm}^{-1}$ which is lower than $2.25 \times 10^{-2} \text{ S cm}^{-1}$ of the CIP sintered GDC at $p\text{O}_2 = 0.21 \text{ atm}$ at 1000° C . This decrease is a result of larger intergranular spaces and uneven networking in microstructure which lead to higher activation energy and low conductivity.[12]

13. Roy-et-al have studied the strontium doping effect on ionic conductivity and densification of gadolinium doped ceria. To measure the sintering behaviour and sintering temperature regimes doped (Sr-GDC) and undoped GDC green sample undergoes dilatometric measurement. Cubic crystal structure of the sintered sample is analysed through X ray diffraction pattern. Microstructural analysis shows the larger grain size with strontium doping and as compared to GDC (0.028 S/cm) sample there is a significant threefold rise in the ionic conductivity of (Sr-GDC) i.e. 0.072 S/cm. This increase in the total conductivity can be due to better densification and increase grain size. Strontium doping not only increase the oxygen ion mobility but decrease the lattice binding energy which leads to lower activation energy. Thus, co-doping is the effective way to find the materials with high ionic conductivity and thus can lessen the cost of fabrication for the manufacture of the solid oxide fuel cell. [13]
14. A.Arabacı-et-al reveals the synthesis of $\text{Nd}_{0.20}\text{Gd}_x\text{Ce}_{0.8-x}\text{O}_{1.9-x/2}$ where ($x = 0, 0.05, 0.10, 0.15, 0.20$) (NGDC) electrolyte by polyol method in which triethylene glycol. At low calcination temperature of 600° C a single phase of fluorite is obtained. The relative density is more than 93% of most of the prepared electrolyte material synthesised at sintering temperature of 1400° C . From the study of x ray spectroscopy of NGDC it is clear that all of them are prepared in a single phase which has a highly pure phase. There is an increase in the relative density and then show a decrease with increase in Gd^{3+} additive ratio. A two probe Ac impedance spectroscopy study the total ionic conductivity in the temperature range of $500\text{-}800^\circ \text{ C}$. which reveals that ionic conductivity can increase with the addition of minor amount of Gd^{3+} cation into solid solution of $\text{Nd}_{0.20}\text{Gd}_x\text{Ce}_{0.8-x}\text{O}_{1.9-x/2}$. [14]
15. M.Choolaei-et-al show the synthesis of GDC nanocrystal by means of a low cost, environment friendly and single step method with the help of a green and novel

participant, ammonium tartrate. The calcination of the obtain precipitate was done at 400 and 600 °C. characterization technique includes FTIR, STEM, XRD, TG/DSC, FESEM AND Raman spectroscopy. At low calcination temperature there is a formation of a single-phase fluorite structure, the same was analysed by XRD and Raman spectroscopy and FESEM and STEM confirmed the crystallite size < 20nm. There is a formation of qausi-spherical particle whose size is in the range of 10-30nm. This study reveals effects of process variables on the properties of dopant metal oxide powder synthesised using carboxylate method.[15]

16. Konysheva-et-al studies the effect of chromium oxide electrochemical and transportation properties of $Ce_{0.9}Gd_{0.1}O_2$. After the spontaneous of absorption of chromium containing molecules of gas phase the electrochemical properties as studied. After mixing the solid oxide electrolyte with chromium (III) oxide $Ce_{0.9}Gd_{0.1}O_2$ based chromium compositions is obtained which aid in the study of transportation properties. It is found that during the absorption of chromium from gas phase it reduces electrolyte surface. It is found that above 735 °C the presence of chromium will weaken the transportation properties of the electrolyte which is due to chromium incorporation and surface microheterogeneity of chromium on electrolyte surface. As a result of this the electric conductivity of the prepared composition is found to exceeds that of the initial solid oxide electrolyte which can be assumed due to change in transportation properties on electrolyte surface and its grain boundaries.[16]
17. S.Taub-et-al studies how the electrical properties of GDC is affected by the transition metal dopants (Co and Cr). For GDC Co and Cr effective sintering agent and Cr will enhance the density of the electrolyte material GDC. There is an isolation of these transition metals at grain boundaries and as second phase precipitate at triple grain junction after sintering. There is an increase in the grain boundaries intrinsic conductivity with 2% addition of Co while even the low concentration of Cr reduces the grain boundaries intrinsic conductivity. Thus, it is found that there the change in conductivity both ionic and electrical is negligible for both Co and Cr which can be due to change in surrounding space charge region and boundary chore electrical potential.[17]
18. G.D.Agli-et-al prepare the nanosized GDC powder by hydrothermal treatment. The precursor used is coprecipitate in the company of different mineralizer solutions. Characterization of the prepared powder includes TEM, SEM, XRD and the thermal analysis. AC impedance spectroscopy of the pellet analyse the electrical behaviour. A

cubic fluorite structure is obtained. These powders independent of the mineralizer solution can fabricate very dense ceramics in an optimized sintering cycle while there is a great impact of the mineralizer solution on the electrical properties of the prepared powder. The higher electrical conductivity is shown by the sample synthesized in neutral and alkali solution. The as synthesized coprecipitate upon hydrothermal treatment can leads to high degree of densification with an optimized sintering cycle without drying step.[18]

19. M. Morale-et-al have studies GDC electrolyte based single chamber fuel cell with electrodes on it. Electrolyte of thickness 200 microns is prepared and then characterized. The fuel here use is a mixture of methane and air. From acetyl-acetate sol-gel method the powder is prepared. Precursor powder of NiO and GDC with varying particle sizes and composition was use to prepare ink which was further analysed and use to obtain optimal porous anode thick films. $\text{La}_{0.5}\text{Sr}_{0.5}\text{CoO}_3$ cathode was prepared which is deposited on the other side of electrolyte. Using dip coating and commercial resins where the electrolyte powder is dispersed both the electrodes both electrolytes were deposited at different thickness range of 20-30 microns. below the direct combustion limit single chamber reactor identifies sand measure the electrical properties and the result was a stable current density which were determine by the temperature, composition and flux rate values of the carrier gas.[19]
20. D.h.Prasad-et-al find that by using the co-firing of all the cell components with the single step the fabrication process can be greatly influence by lowering the sintering temperature of the solid oxide fuel cell. The powder is prepared here is synthesis by co-precipitation method at room temperature. Characterization analysis of the prepared powder includes Raman spectroscopy, X ray diffraction (XRD) and transmission electron microscopy (TEM). From dilatometry studies the relative density of the prepared powder is more than 97% at a relatively low sintering temperature of 950° C. Ionic conductivity comes out to be 1.64×10^{-2} S/cm at 600 °C makes it suitable for intermediate temperature solid oxide fell cell (IT-SOFCs) [20]

REFERENCES

1. Aliye Arabacı, n, M.Faruk Oksuzomer, Preparation and characterization of 10mol% Gd doped CeO₂ (GDC) electrolyte for SOFC application, *Ceramics International*, 2012, 38, 6509-6515
2. K.C. Anjaneya, Mahander Pratap Singh, Synthesis and properties of gadolinium doped ceria electrolyte for IT-SOFCs by EDTA-citrate complexing method, *Journal of Alloys and Compounds* 695, 2017, 871-876.
3. Aleksej Zarkova, AndriusStanulisa, Tomas Salkus, Algimantas Kezionis, Vitalija Jasulaitiene, Rimantas Ramanauskas, Stasys Tautkus, Aivaras Kareiva, Synthesis of nanocrystalline gadolinium doped ceria via sol–gel combustion and sol–gel synthesis routes, 2016, 3972–3988.
4. Jie Yang, Bifa Ji, Jingyu Si, Quanzheng Zhang, Qiyi Yin, Jingsong Xie, Changan Tian, Synthesis and properties of ceria-based electrolyte for IT-SOFCs, *International Journal of Hydrogen Energy* 41, 2016, 15979-15984.
5. Siti Munira Jamil, Mohd Hafiz Dzarfan Othman, Mukhlis A. Rahman, Juhana Jaafar, Ahmad Fauzi Ismail, Anode supported micro-tubular SOFC fabricated with mixed particle size electrolyte via phase-inversion technique, *International Journal of Hydrogen Energy* 42, 2017, 9188-9201.
6. G. Accardo, L. Spiridigliozzi, R. Cioffi, C. Ferone, E. Di Bartolomeo, Sung Pil Yoon, G. Dell’Agli, Gadolinium-doped ceria nanopowders synthesized by urea-based homogeneous co-precipitation (UBHP), *Materials Chemistry and Physics* 187, 2017, 149-155.
7. Eun-Hui Hyeong, Seung-Muk Bae, Chan-Rok Park, Jong-Sung Park, Young-Sung Yoo, Hee-Sun Yangand, Jin-Ha Hwanga, Sonochemical synthesis of highly sinterable/nanocrystalline CeO₂-based electrolyte powders for intermediate-temperature solid oxide fuel cells, *Journal of Ceramics Processing Research* 13, 2012, 349-352.

8. J. Chandradass, Baekil Nam, Ki Hyeon Kim, Fine tuning of gadolinium doped ceria electrolyte nanoparticles via reverse microemulsion process, *Colloids and Surfaces* 348, 2009, 130-136.
9. Hari Prasad Dasari, Kiyong Ahn, Sun-Young Park, Jongsup Hong, Hyoungchul Kim, Kyung Joong Yoon, Ji-Won Son, Byung-Kook Kim, Hae-Weon Lee, Jong-Ho Lee, Record-low sintering-temperature (600 C) of solid-oxide fuel cell electrolyte, *Journal of Alloys and Compounds* 672, 2016, 397-402.
10. Ieeba Khan, Pankaj K. Tiwari, Suddhasatwa Basu, Development of melt infiltrated gadolinium doped ceria-carbonate composite electrolytes for intermediate temperature solid oxide fuel cells, *Electrochimica Acta* 294, 2019, 1-10.
11. Hikmet Okkaya, Mahmut Bayramoglu, M.Faruk Oksuzomer, Ultrasound assisted synthesis of Gd and Nd doped ceria electrolyte for solid oxide fuel cells, *Ceramics International* 39, 2013, 5219–5225.
12. Chanjin Son, Aman Bhardwaj, Jaewoon Hong, Jin-Wook Kim, Heung-Soo Moon, Hyo-Seop Noh and Sun-Ju Song, Plasma-sprayed gadolinium-doped ceria (GDC) for intermediate temperature solid electrolyte, *Journal of Ceramic Processing Research* 18, 2017, 858-864.
13. Roy, Buchi Suresh M. & Johnson, the effect of strontium doping on densification and electrical properties of $Ce_{0.8}Gd_{0.2}O_{2-\delta}$ electrolyte for IT-SOFC application, *Ionics* 18, 2012, 291-297.
14. Aliye Arabacı, Tuba Gurkaynak Altıncekic, Mehtap Der and Mehmet Ali Faruk Oksuzomer, Preparation and properties of ceramic electrolytes in the Nd and Gd Co-Doped ceria systems prepared by Polyol Method, *Journal of Alloys and Compounds*, 2019, 1-29.
15. Mohammad Mehdi Choolaei, Qiong Cai, Robert C.T. Slade, Bahman Amini Horri, Nanocrystalline gadolinium-doped ceria (GDC) for SOFCs by an environmentally-friendly single step method, *Ceramics International* 44, 2018, 13286-13292.
16. Konysheva, E. Yu., The Effect of Chromium Oxide on the Conductivity of $Ce_{0.9}Gd_{0.1}O_2$ a Solid-Oxide Fuel Cell Electrolyte, *Russian Journal of Electrochemistry* 54, 2018, 544-553.

17. Samuel Taub, Kerstin Neuhaus, Hans-Dieter Wiemhofer, Na Ni, John A. Kilner, Alan Atkinson, The effects of Co and Cr on the electrical conductivity of cerium gadolinium oxide, *Solid State Ionics* 282, 2015, 54-62.
18. Gianfranco Dell'Agli, Luca Spiridigliozzi, Antonello Marocco, Grazia Accardo, Claudio Ferone, Raffaele Cioffi, Effect of the mineralizer solution in the hydrothermal synthesis of gadolinium-doped (10% mol Gd) ceria nanopowders, *Wichtig Publishing*, 2016, 189-196.
19. M. Morales, S. Pinola, M. Segarrab, Intermediate temperature single-chamber methane fed SOFC based on Gd doped ceria electrolyte and $\text{La}_{0.5}\text{Sr}_{0.5}\text{CoO}_{3-\delta}$ as cathode, *Journal of Power Sources* 194, 2009, 961-966.
20. D. Hari Prasad, H.-R. Kim, J.-S. Park, J.-W. Son, B.-K. Kim, H.-W. Lee, J.-H. Lee, Superior sinterability of nano-crystalline gadolinium doped ceria powders synthesized by co-precipitation method, *Journal of Alloys and Compounds* 495, 2010, 238-241

CHAPTER 3

EXPERIMENTAL DETAILS

3.1 Synthesis of GDC (electrolyte) material

Cerium (III) nitrate hexahydrate ($\text{Ce}(\text{NO}_3)_3 \cdot 6\text{H}_2\text{O}$ 99%, Sigma Aldrich) and Gadolinium (III) nitrate hydrate ($\text{Gd}(\text{NO}_3)_3 \cdot \text{H}_2\text{O}$ 99.9%, Alpha Aesar) were used as metal precursor. Ethylene glycol ($\text{C}_2\text{H}_6\text{O}_2$ 99%, Loba Chemie) and Citric acid $\text{C}_6\text{H}_8\text{O}_7$ 99%, Loba Chemie) were used for the polymerization to take place. Both Metal precursors were dissolved in distilled water. Citric acid (anhydrous) was liquified in distilled water and after that it is added to the metal precursor solution. The molar ration of total oxide: citric acid and ethylene glycol: citric acid was chosen as 2:1 and 4:1 respectively. After the entire solution become homogeneous it was kept on the hot plate and the temperature was raised to $100\text{ }^\circ\text{C}$ for 5-6 hours with continuous at this temperature. During this period the colour of the solution was changed from transparent white to light brown and a foam like gel was obtained. Further, the magnetic stirrer was removed and temperature was lowered down to nearly $60\text{-}80\text{ }^\circ\text{C}$ and kept to overnight till this foam get converted into light yellow colour powder. TGA/DTA inspects the thermal behaviour of $\text{Ce}_{0.9}\text{Gd}_{0.1}\text{O}_{1.95}$ powder from room temperature to $800\text{ }^\circ\text{C}$ at $5\text{ }^\circ\text{C min}^{-1}$ heating rate with N_2 or air as medium. The crystal structure of the crystalline phases was determined by x-ray diffraction technique. Panalytic X'pert pro MRD with scanning range from $10\text{-}90^\circ$ with step size $0.001^\circ/10\text{sec}$ was used. The surface morphology was studied using scanning electron microscope SEM (Model: JSM-6510/6460LV, JEO). An auto fine coater (Model: JEC-3000FC) is used to make thin layer of platinum. AC Impedance analyser (1260A Impedance/Gain-Phase Analyzer) was used measure the ionic conductivity of the sintered GDC pellets.

The theoretical density GDC is 7.2g/cm^3 . GDC pellets were formed in a form of circular disk by hydraulic press with a pressure of 5 kg/cm^2 for pellet with diameter 10mm . Further the sample were sintered at $1250, 1350, 1450\text{ }^\circ\text{C}$ for 6hrs with an intermediate step at $100\text{ }^\circ\text{C/1hr}$. The density of the calcined powder $\text{Ce}_{0.9}\text{Gd}_{0.1}\text{O}_{1.95}$ at $1000\text{ }^\circ\text{C}$ which pressed to disk at 5 kg/cm^2 with hydraulic press and then sintered at $1250, 1350, 1450$ for 6 hrs with a heating rate of $5\text{ }^\circ\text{C/min}$. were determined by the Archimedes' method;

$$D_{rs} = W_{obj} \text{ g} / W_1 - W_2$$

Where, W_{obj} = dry weight, W_1 = wet weight (water in the body), W_2 = body's weight in air, ρ = density of the solvent

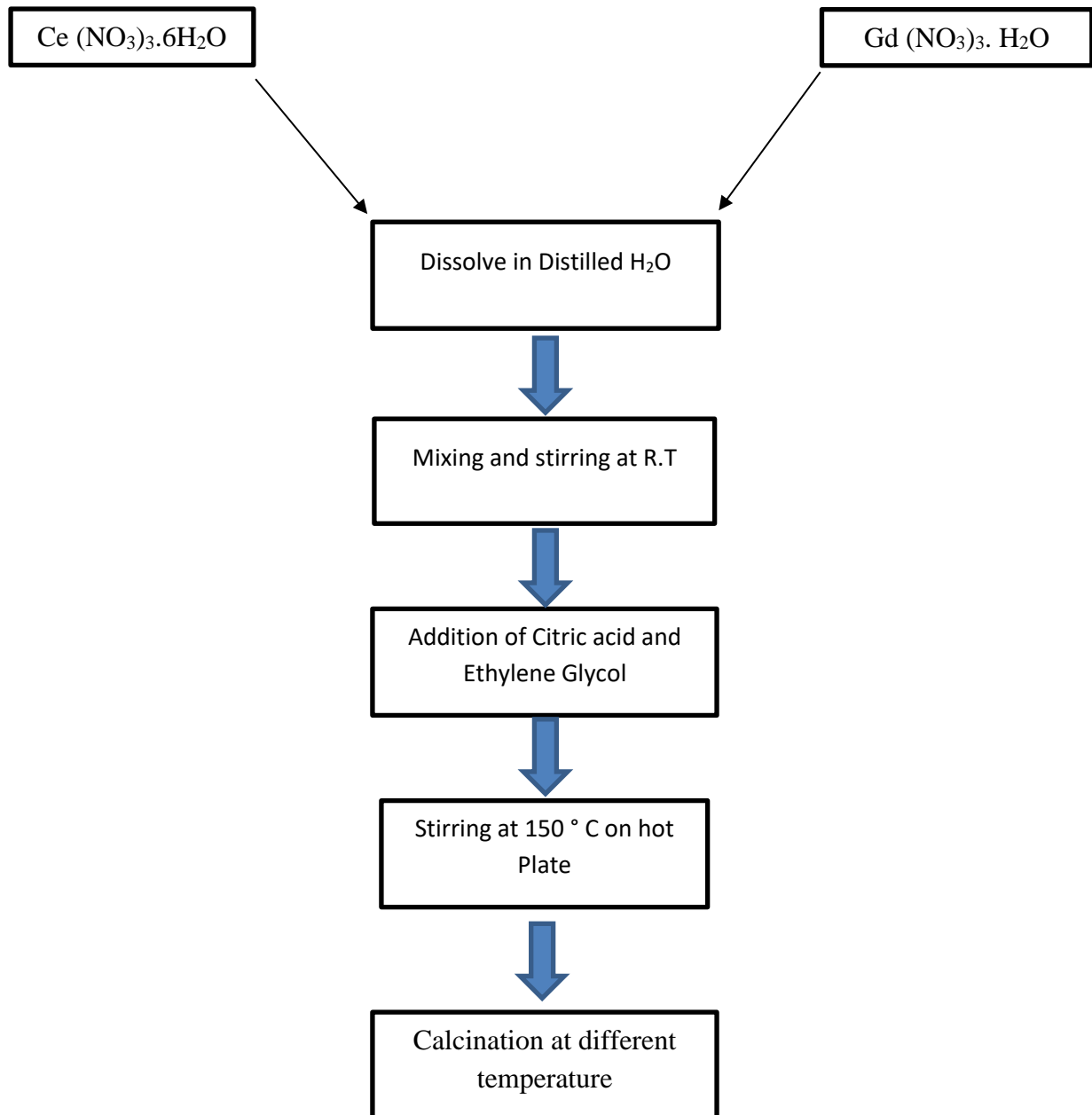


Fig 3.1 Flowchart of the synthesis process of $Ce_{0.9}Gd_{0.1}O_{1.95}$ via sol gel process

Plan of Work

- Aim:**
1. To prepared the electrolyte composition $Ce_{0.9}Gd_{0.1}O_2$ via Sol-gel method.
 2. To perform conductivity and cell test of GDC pellet sintered at 1250, 1350, 1450 °C

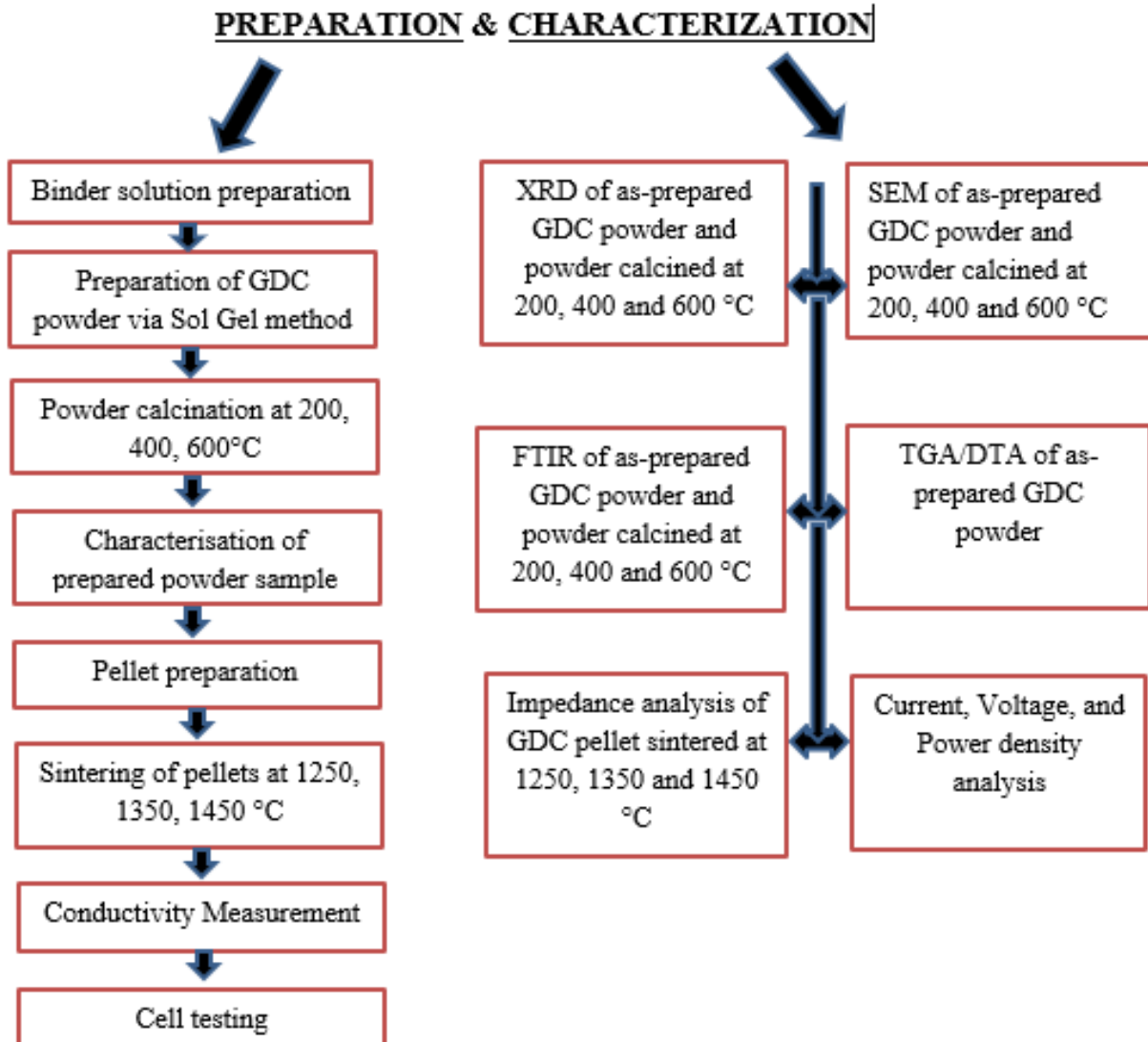


Fig 3.2 Flow chart for the plan of work

3.2 Binder Solution Preparation

Addition of binder is very important in making ceramic pellets to achieve high green density (~60% of theoretical density). The binder solution used for the preparation of the GDC pellet was made of PVA (MW. ~10000) (Poly Vinyl Alcohol) solution. PVA solution is prepared by

taking the 2-5 wt.% of PVA to the distilled water i.e. (for a 5 wt.% solution, 5 gm of PVA powder in 95 ml of water). Solution was then placed on a hot plate with continuous stirring using a magnetic stirrer. The solution must be stirred continuously until the solution became clear. Temperature can be set to 50 °C for fast dissolution of the PVA in distilled water. A cone like shape must be appear in the beaker while stirring. PVA act as a binder that holds the GDC-10N (10 wt.% Gd doped in Ce of fuelcellmaterials.com) Nano particles. For a 40 ml of distilled water the 5 wt.% is 2 grams thus we must take 38 ml of distilled water and add 2 ml of PVA in it. For making the GDC pellet we need to add 2 wt.% of the PVA solution in the powder. To make pellets in laboratory scale take a small amount of powder (10-15 gm) to be pelletised in agate mortar (5-6-inch diameter is better) and using dropper pour few drops (5-10) of PVA solution on it. Grind the powder until a fine powder is obtained using pestle. This process may be repeated to eliminate agglomeration which depend upon the type and fineness of the powder to be pelletise. Now powder is ready for making pellets It is very important to take a note of edges of pellet i.e. if the added PVA quantity is less than there is a chance that the pellet will be cracked from the edges and its large quantity may be attributed to the layering of the central and middle region of the pellet. A few minutes drying of the prepared powder can eliminate this problem.

3.3 Pellet formation

The theoretical density of GDC is 7.2g/cm³. The amount of powder required for making a pellet of desire thickness is as follow. First calculate the radius of the die (let's take in my case is 5mm). And we are required to make a pellet of thickness 1 mm, (for a pellet of 1 mm thickness calculate the volume taking the thickness slightly greater that the required value as some of the thickness is removed during the polishing of the pellet. In my case I take the thickness of around 1.2 mm) then the volume is calculated as: -

$$\text{Volume} = \pi r^2 h$$

where, $\pi = 3.14$, r = is the radius of the die, h = is the required height/thickness of the pellet.

According to the above calculation the volume comes out to be 0.094 cm³. Now we know that

$$\text{Density} = \text{Mass}/\text{Volume}$$

$$\text{Density of GDC} = 7.2\text{gm}/\text{cm}^3$$

$$\text{Volume calculated} = 0.0094 \text{ cm}^3$$

Thus, from this mass of GDC required for palletisation is 0.678gm.

Weight the powder sample correctly at least up to 3 decimal places. Pellets of thickness 1.2mm is made by uni-axial compression in a stainless-steel die of diameter 10mm with a

pressure of $5\text{kg}/\text{cm}^2$. The pellets thus fabricated were sintered at $1250\text{ }^\circ\text{C}$, $1350\text{ }^\circ\text{C}$, $1450\text{ }^\circ\text{C}$ for 6 hours. The heating rate was set at $2\text{ }^\circ\text{C}$ per minute. The sacrificial layer of same powder is kept beneath the GDC pellet to avoid other chemical reaction during sintering. Same calculation was used for the big pellet of 30mm diameter and 0.5mm thickness. Pressure applied during the palletisation is around 5 tons.

3.4 Phase analysis.

X-ray diffraction (XRD) technique was employed for the characterisation of the sintered sample. X-ray diffraction (XRD) studies was carried out on powders using PAN analytical X'pert PRO MRD with a scanning range of $10\text{-}90^\circ$ with a scanning rate of $0.001^\circ/10\text{sec}$. Reitveld modification of the XRD data was performed using BRASS for unit cell volume and composition evaluation. The parameters for CeO_2 (fluorite Fm3m) was used as the starting structural models for modification in the software.



Fig 3.3 X'PERT MRD powder X-Ray Diffractometer

3.5 Microstructural analysis

Pellets were polished using emery paper of 600,800, 1000, 2000 successively before observation for using scanning electron microscopy (SEM) (Model: JSM-6510/6460LV, JEO). An auto fine coater (Model: JEC-3000FC) was used for sputtering the samples with platinum. Thermal etching was done at a temperature $100\text{-}200\text{ }^\circ\text{C}$ less than the sintering temperature for

2 hours. The SEM images of all the sample were analysed to find out the grain size and the presence of the porosity in the sample.



Fig 3.4 Scanning Electron Microscope used to study the surface morphology of GDC

3.6 Impedance analysis

The Ametek 1260A Impedance/Gain-Phase Analyzer was used for the measurement of Gadolinium Doped ceria (GDC) pellets sintered at 1250 °C, 1350 °C, 1450 °C. Impedance analyser was run using a program inscribed in SMART Impedance measurement software. The frequency range was set to 1kHz to 10MHz for a temperature range from 100 °C- 500 °C with an applied potential of 1V. When Ac voltage is applied to a material either in solid or liquid form, current will pass this. The ration of voltage to current is known as the Impedance as the frequency of the applied voltage varies the measured impedance varies which is linked to the properties of solid or liquid. This may be due to the physical structure, chemical process or combination of both.



Fig 3.5 Impedance analyser used for dielectric measurement

3.7 TGA (Thermogravimetry Analysis)

The thermal behaviour of the sample is examined by Thermogravimetry technique. It inspects the variation in the weight loss or gain in a substance with change in time or temperature. Isothermal mode comes to exist when the weight is changed with time. It is one of the most important characterization technique for the thermal analysis of the material. The TGA employs the very elementary principle of change in mass of the sample. The main events which studied by the thermal analysis are oxidation, adsorption, absorption, desorption, etc. It is also used to learn about the gaseous or volatile products vanished when sample undergo some chemical reactions. It also provides a measure for the thermal stability of the samples. The factors that influencing the change in mass can be attributed to the physical form of sample, nature of environment used for analysis, shape of the sample holder and the rate at which heating and cooling occur. The configuration of the TGA analyser with specification (a) temperature range ambient to 1500 ° C, (b) air atmosphere, (c) 0.1µg balance sensitivity, (d) sample pans of alumina and platinum is shown in fig; 3-6



Fig 3.6 Thermogravimetry Analyser (TGA)

3.8 Fuel Cell test

A Probostat™ sample holder (Fig 3-7 (a) & (b)) was used for testing conductivity as well as the cell. Testing the cell measure the cell voltage with variation in current. The diameter of pellet is approx. 22 mm and the thickness are around 1.24mm. This silver paste (as cathode and anode) is applied over 20mm diameter (which act as cathode) on one side and 16mm diameter (which act as anode) on the other side of the pellet and is heated at 500 °C for 2-3 hrs .The

support tube was an alumina tube with inner diameter of 14mm and outer diameter of 19 mm . Mica washer was used as a sealant with inner and outer radius 12.50 mm and 18.85mm approx. respectively. Gold mesh was employed as a current collector for both the electrodes. The function of leads was carried forward by platinum wire in contact with the current collector. The sealing and electrical contact were stiffened by a spring-loaded assembly ensures the electrical contact and proper sealings. A button cell electrolyte supported SOFC is placed above the mica washer on the top of the alumina support tube. The current collecting gold mesh was soldered to the platinum wire. A proper leak check examination must be done to prevent any type of gas leakage. After this, entire setup was to kept inside a vertical tube furnace. A chromel alumel thermocouple must be kept near the sample to record the temperature. Hydrogen was supplied at various flow rates to anode chamber and cathode was exposed to air/oxygen. The I-V characteristics were obtained using AMREL eload Virtual panel software of National Instruments.

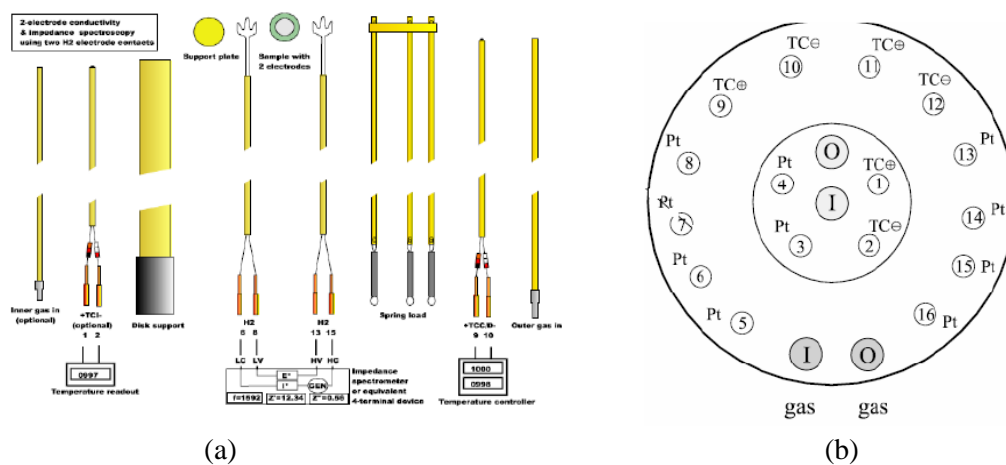


Fig 3.7 (a) shows the schematic assembly of Probostat™ component for fuel cell measurement and (b) shows the schematic assembly of Probostat™ base unit

4.1 Structural analysis

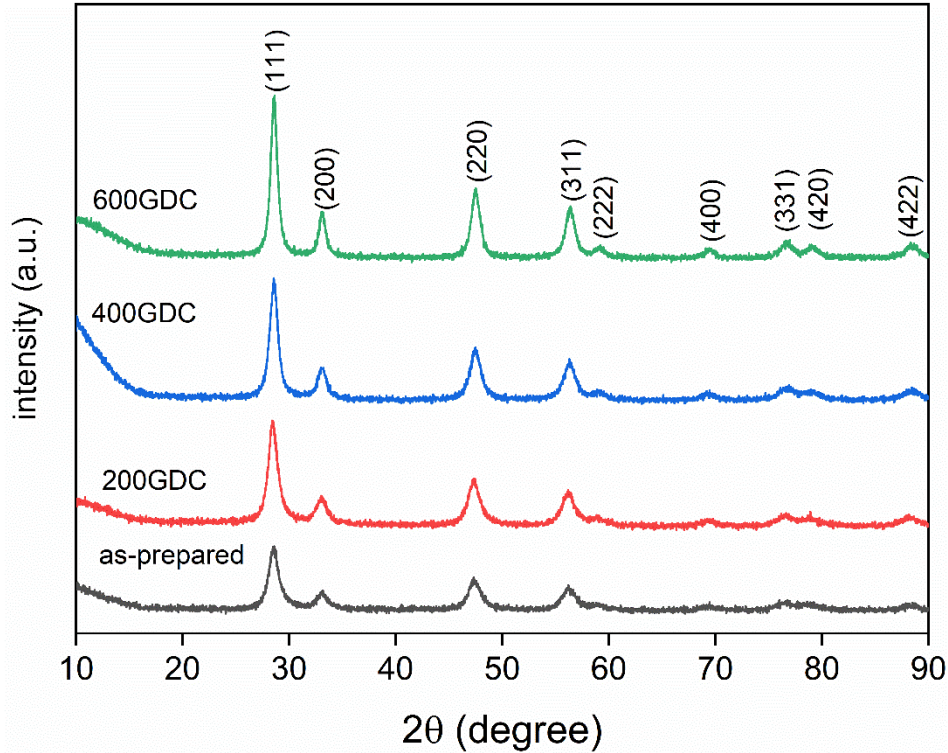


Fig 4.1 XRD pattern of as prepared sample & GDC powders calcined at 200, 400, 600 °C for 2hrs in air

Fig. 4.1 represents x-ray diffraction patterns for as-synthesized and GDC powder calcined at 200, 400 and 600 °C. There are multiple peaks observed corresponding to the cubic fluorite structure of $\text{Ce}_{0.9}\text{Gd}_{0.1}\text{O}_2$ which matches with the standard card ICDD-01-075-0161 (space group=Fm-3m, space group number=225). The peaks (400), (331), (420) are absent in as-prepared sample however they begin to resolve with an increase in calcination temperature. The broadness and intensity of the peak (111) increases with increase in calcination temperature which leads to decreasing crystallite size of the samples. From the Debye-Scherrer formula [3], the crystalline size of the as-prepared and 200GDC, 400GDC, 600GDC sample is in the range of 93 to 119 Å. The crystallite size (97 Å) is minimum for the 200GDC and maximum (1 Å) for 600GDC sample. The sample with high crystallinity is synthesized at 600 °C without any residue. There is no secondary peak in the XRD pattern, confirms the phase purity.

Table 4.1 Crystallite size and lattice strain for GDC synthesised by sol-gel meth

Sample label	FWHM (obs.)	Pos. (2 θ)	Crystallite size (\AA)	Lattice strain (%)
as-prepared	0.9036	28.520	91	1.740
200GDC	0.8466	28.429	97	1.459
400GDC	0.8169	28.540	100	1.402
600GDC	0.7082	28.557	116	1.214

4.2 FTIR analysis

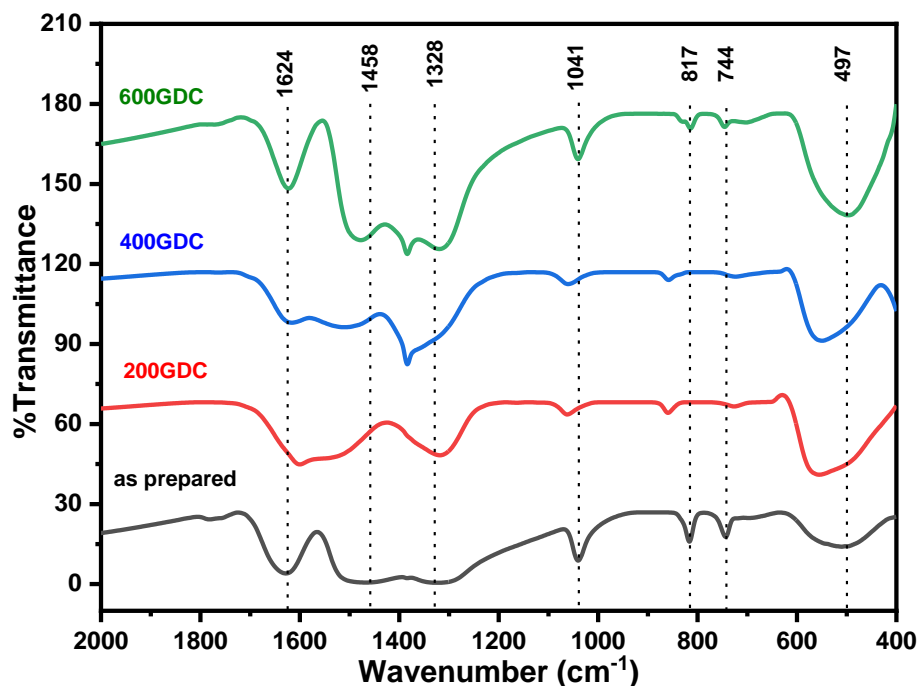
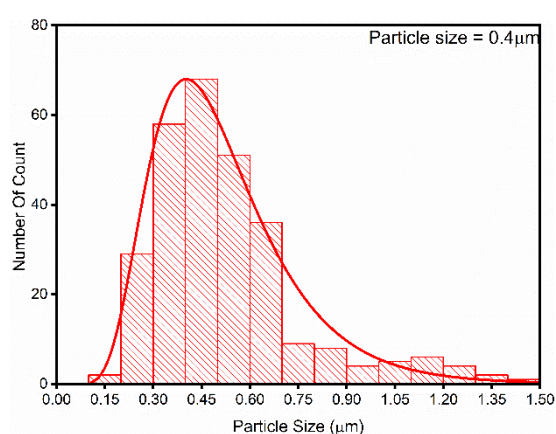
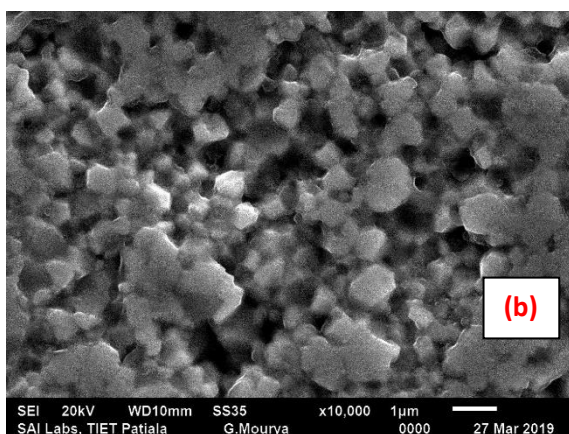
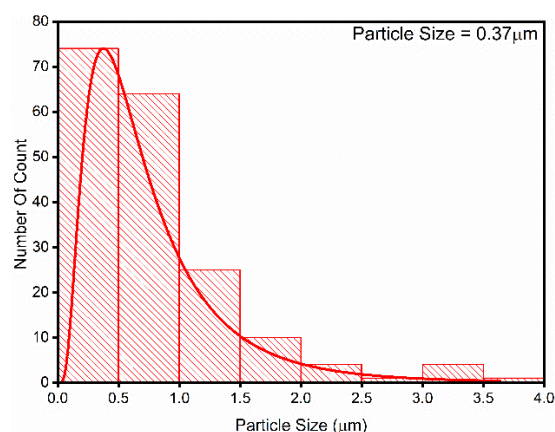
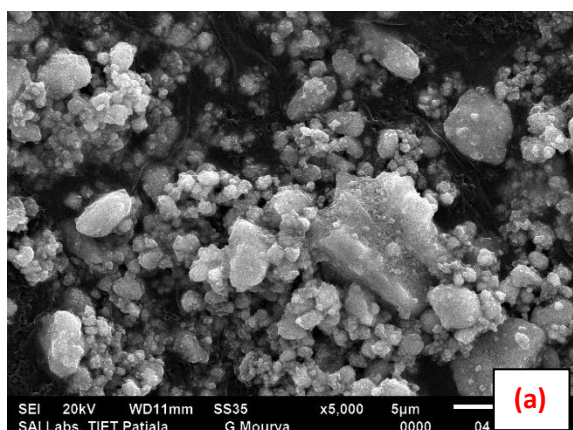


Fig 4.2 FTIR spectra of as-prepared GDC powders and calcined powder at 200, 400, 600°C

It is depicted in Fig .4.2., the FTIR spectra of as-prepared and calcined GDC powders at 200, 400, 600 °C temperature. The peaks are observed at 1624, 1458, 1328, 1041, 817, 744, 497 cm⁻¹

¹. The presence of COO⁻ vibration (the carboxylate salt group) is assigned to the peak in the nearby region of 1624 cm⁻¹[1]. The peak at 1328 cm⁻¹ represents the characteristic absorption of the nitrate ion where peak at 1041 cm⁻¹ is attributed to the asymmetric stretching of C-O bond. It is observed that the peak at 1458 cm⁻¹ resolves with increase in calcination temperature and are shifted to the lower frequency side which is a results of CO₂ reaction with the nitrates to form carbonate phase during the synthesis. The peaks at 817 cm⁻¹ are related to the presence of Ce-O bond vibrations. The presence of the metal oxide bonds in the spectra can be ascribed by the broad absorption band in range 400-650 cm⁻¹[4].

4.3 Surface Morphology



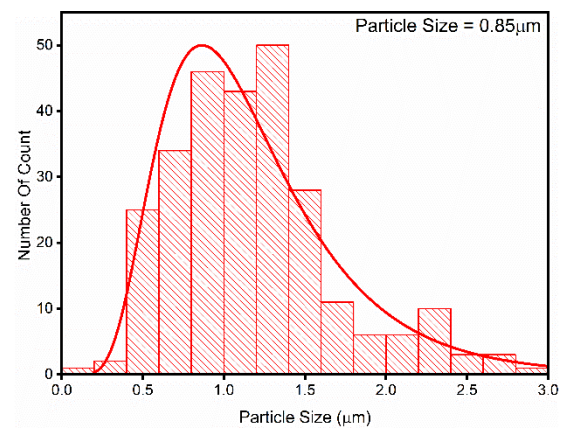
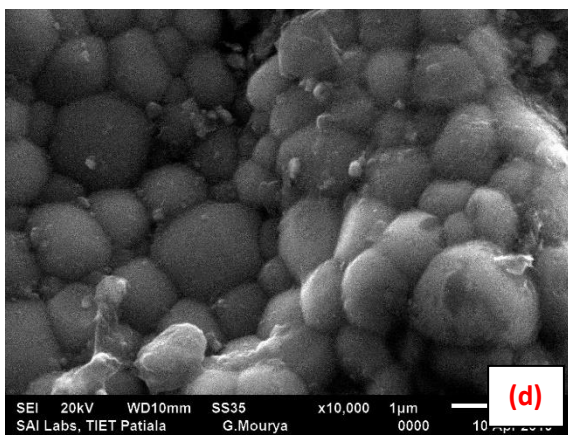
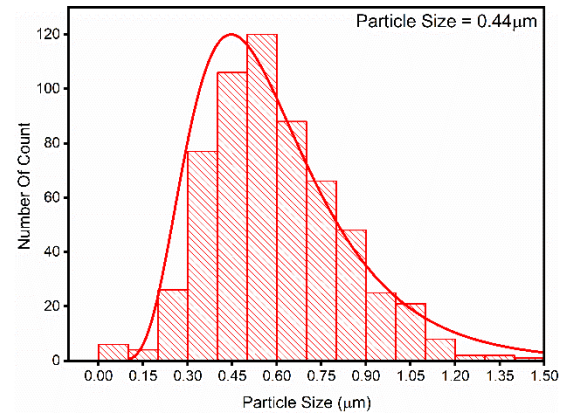
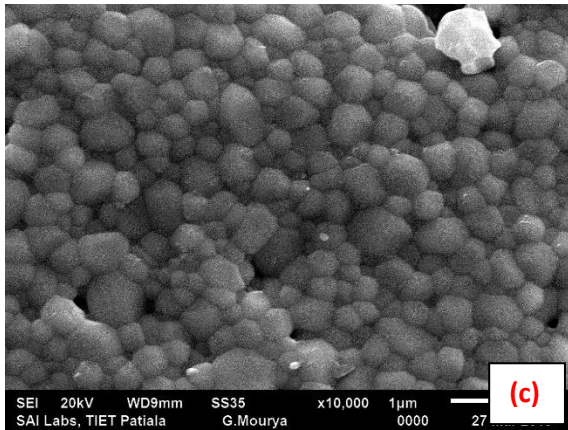


Fig 4.3 (a) SEM micrograph of surface of GDC samples calcined at 600 °C for 2h (5000x) and GDC sample sintered at (b) 1250 °C, (c) 1350 °C and 1450 °C for 6 h (10000x)

Fig 4.3(a). reveals SEM image of the calcined GDC ($\text{Ce}_{0.9}\text{Gd}_{0.1}\text{O}_{1.95}$) powder along with histogram which calculate the average size of the GDC particles at 600 °C calcination temperature for 2h. It can be clearly seen from the micrograph Fig 4.3 (a) that the average size of the as prepared powder particles is around 0.37 µm. Fig 4.3 (a), (b), (c) represent SEM image of the sintered pellets of GDC at 1250 °C, 1350 °C, 1450 °C respectively. From the histogram study it is revealed that the average size of grains for pellet sintered at 1250 °C, 1350 °C, 1450 °C is 0.4 µm, 0.44 µm, 0.85 µm respectively. Thus, it may be concluded that the size of the grain is directly proportional to the sintering temperature i.e. as the sintering temperature is increased the size of the grain will increase. It is found that the grains in the pellets sintered at 1450 °C have denser structure with less porosity except some residual pores than the other two samples which leads to a higher total ionic conductivity [5].

4.4 Thermal Analysis

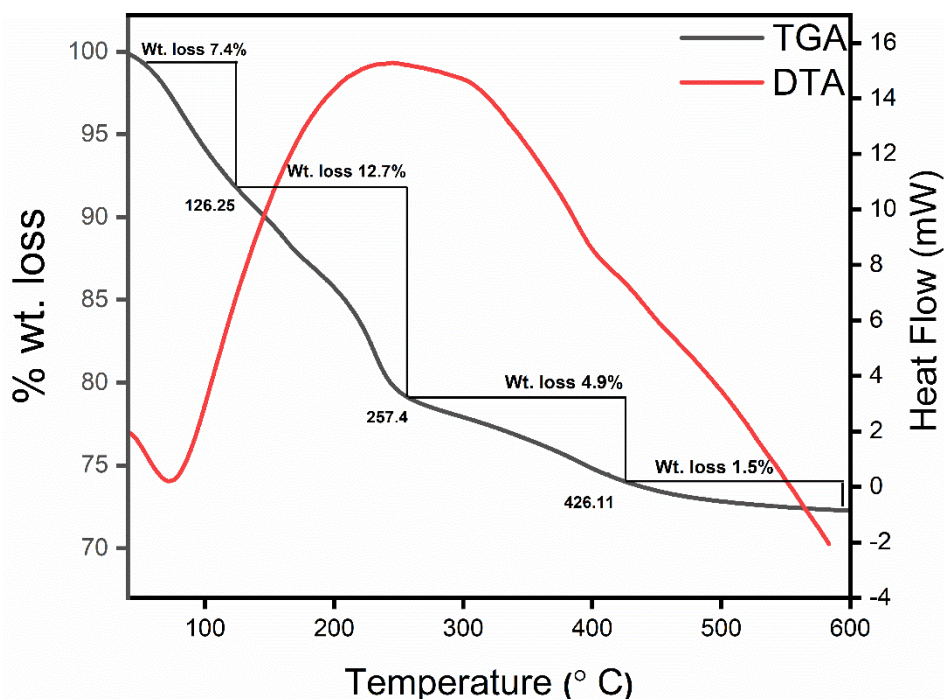


Fig 4.4 TGA and DTA thermograph of as prepared GDC powder

Fig 4.5 shows the DTA/TGA curve of the as prepared GDC powder (without calcination). As depicted by the TG curve in Fig 4.5, the thermal decomposition of $Ce_{0.9}Gd_{0.1}O_{1.95}$ is a four-step process. The loss of moisture and dehydration of acetate is represented by the first step which shows a weight loss of 7.4% between the temperature range 50 - 126.25 °C. In second step weight loss of 12.7% is observed in the temperature range 126.25 - 257.4 °C which may be attributed to the decomposition of the organic compounds. The main thermal decomposition was observed in the temperature range from 126.25 - 426.11 °C with a total weight loss of 17.6 % which is due to the combustion of the residual organic materials in the sample [1]. This thermal decomposition behaviour in the temperature range 70.25 – 600 °C is assigned to the exothermic peak in the DTA curve which may be attributed to the burning of residual surfactants. The decomposition of the intermediate phase to oxide is given by the fourth step with the final weight loss of 1.5 % at temperature > 426.11 °C. The exothermic peak in the DTA curve is not related to crystallization, thus at room temperature it is an indication of formation of solid solution [2].

4.5 Leakage current study

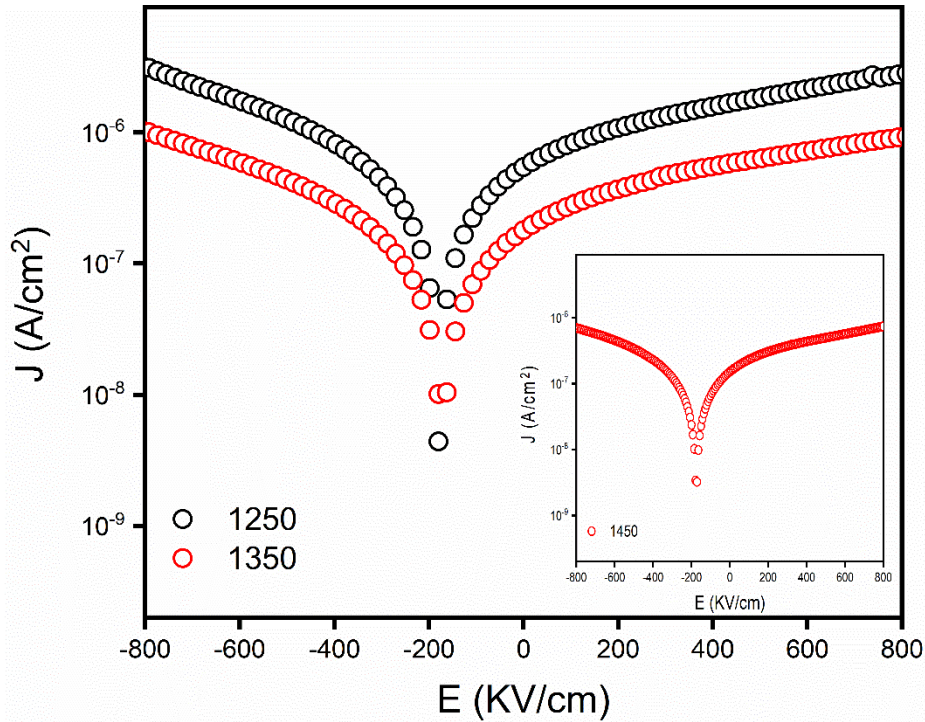


Fig 4.5 Current voltage characteristics of GDC pellets sintered at 1250, 1350, 1450 °C

The behaviour of the leakage current and electric field dependence of leakage current density of GDC pellet sintered at 1250° C, 1350° C and 1450° C is depicted in Fig 4.5. Leakage current density of GDC pellets sintered at 1250 ° C and 1350° C is found to be 4.33×10^{-9} A/cm² and 1.03×10^{-8} A/cm² in an applied voltage field ~ -800 to 800 V [6]. Whereas the leakage current density study of GDC pellet at sintered 1450° C was performed under different experimental conditions and is found to be 2.89×10^{-9} A/cm². The behaviour of the leakage current density is not symmetric as it appears at an applied negative voltage of -200 V.

4.6 Conductivity Measurement

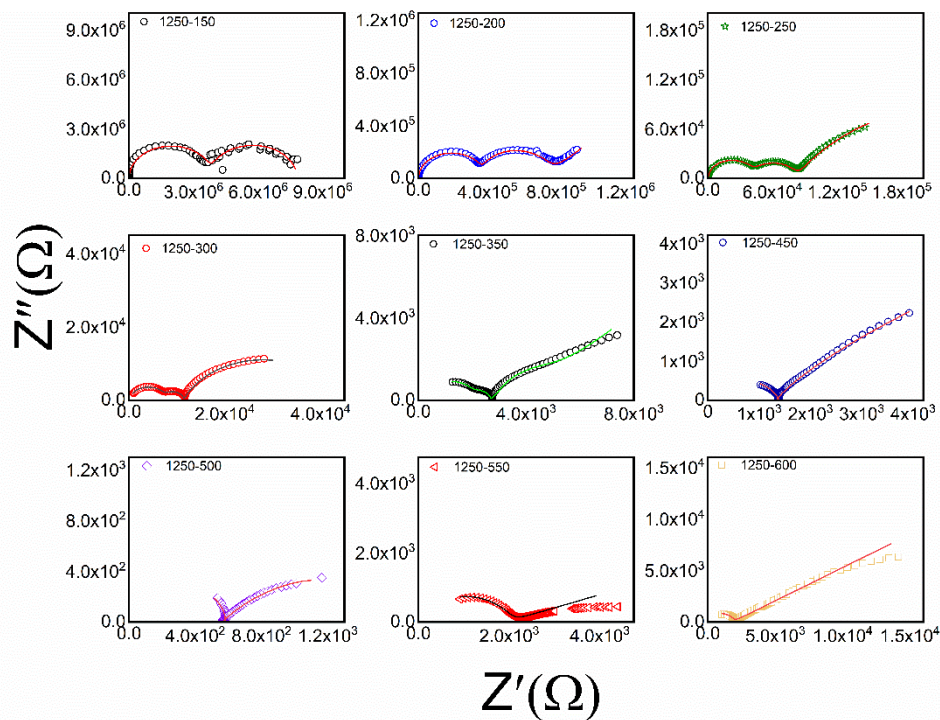


Fig 4.6 Cole-Cole plot of GDC pellet sintered at 1250° C in temperature range from 150-600° C. The fitted data is represented by solid line

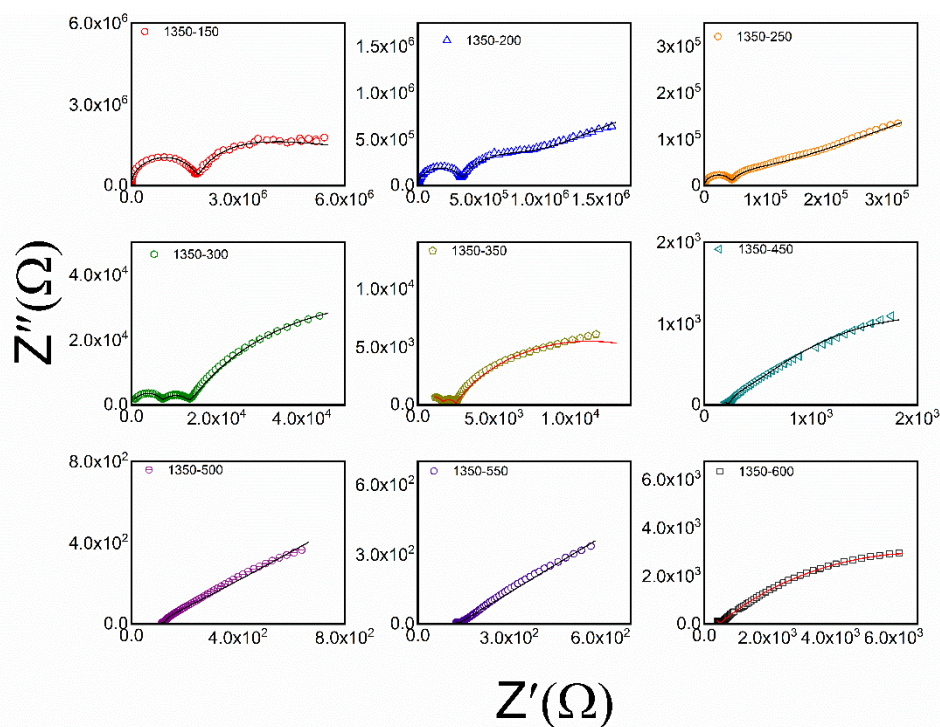


Fig 4.7 Cole-Cole plot of GDC pellet sintered at 1350° C in temperature range from 150-600° C. The fitted data is represented by solid line

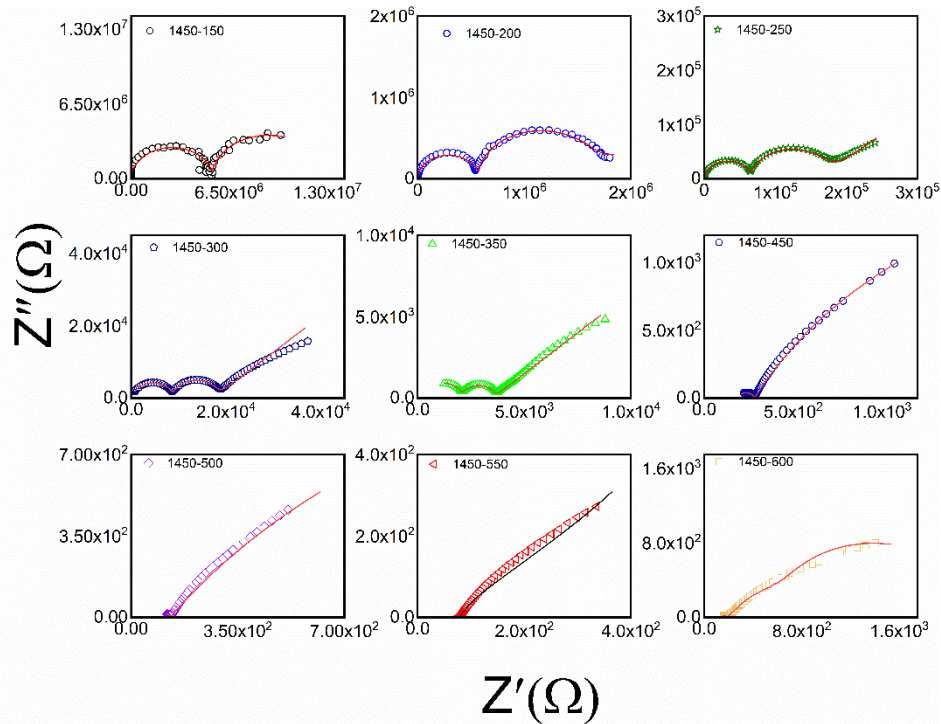


Fig 4.8 Cole-Cole plot of GDC pellet sintered at 1450° C in temperature range from 150-600° C. The fitted data is represented by solid line

Fig 4.6, 4.7, 4.8 represents the Cole-Cole plots of the sintered samples in the temperature range of 150-600° C. Three semi-circles are observed for 1250GDC sample in the temperature range of 200-300° C. After that two semi-circles are observed in the temperature range 350-600° C and at 150° C. For pellet sintered at 1350° C, three semicircles were observed only at 300° C and similar behaviour for 1450 ° C sintering temperature were observed for temperature range 250-350°. This random appearance of three and two semi-circles is a nature dependent property of the sample and depend upon the experimental conditions [7, 8]. Three semi-circles contain contribution of the grain, grain boundary and electrode. The first high frequency semi-circle resembles to the bulk conductivity which is fitted by a comparable circuit in which the bulk resistance R_{grain} and the constant phase element $\text{CPE}_{\text{grain}}$ are connected in parallel [4], whereas the second semi-circle is attributed to the grain boundary contribution in which fitting is done by connecting two circuit in series in which the bulk resistance R_{grain} and the constant phase element $\text{CPE}_{\text{grain}}$ are connected in parallel. The contribution of the electrode-electrolyte interface is represented by third semi-circle corresponds whose fitting is equivalent to the circuit used for second semi-circle but with an additional $\text{CPE}_{\text{electrode}}$ connected in series to it. The total resistance R is the sum of electrode resistance, grain boundary resistance and the bulk resistance, which can be used to describe the total ionic conductivity and favour the grain

boundary blocking effect by van Dijk and Burggraaf [9]. The high resistance accompanying the low grain boundary conductivity is reveals that the grain boundaries act as barrier to the oxygen ion transportation and limit the total ionic conductivity. This effect may be due to the dissolution of some kind of impurities in the grains, its segregation in grain boundaries and when the impurities is present in high concentration. A single semicircle arises when the resistance of grain and grain boundary become independent of frequency which refers the electrode resistance whose contribution to total resistance is maximum [4]. High resistance at electrode-electrolyte interface blocks the oxygen ion transportation beyond the electrode-electrolyte interface.

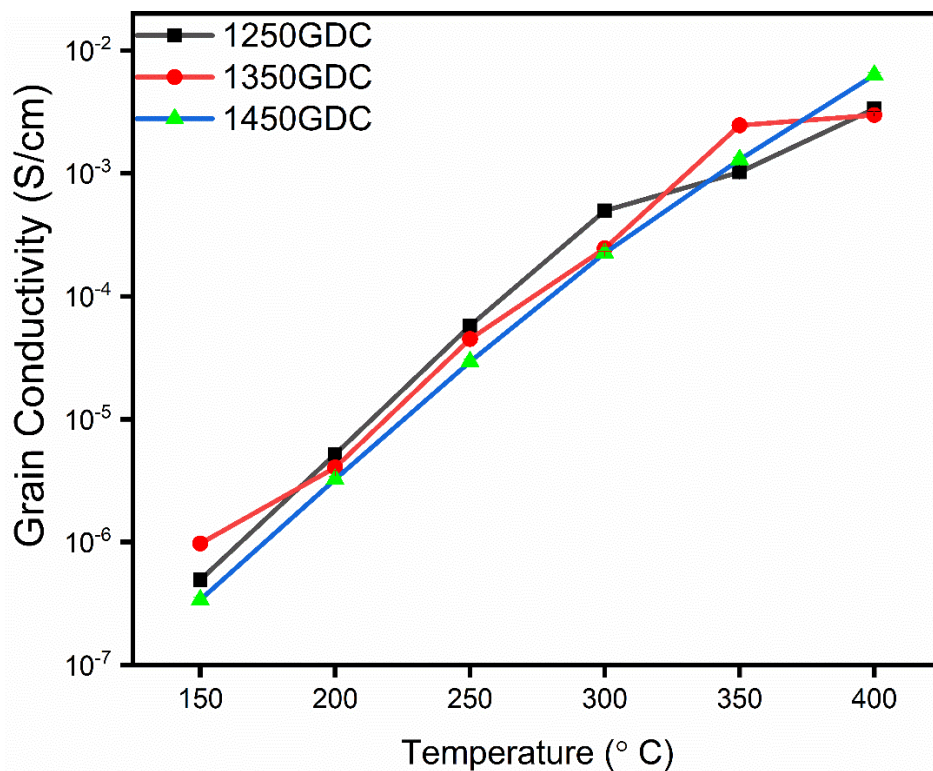


Fig 4.9 Grain conductivity as a function of temperature for all the sample sintered at different temperature

Fig 4.9 show the bulk conductivity with temperature. it exposes a thermally activated process in which the ionic conductivity of bulk conductivity is maximum for the GDC pellet sintered at a relatively high temperature [16].

4.7 Temperature and frequency dependent conductivity

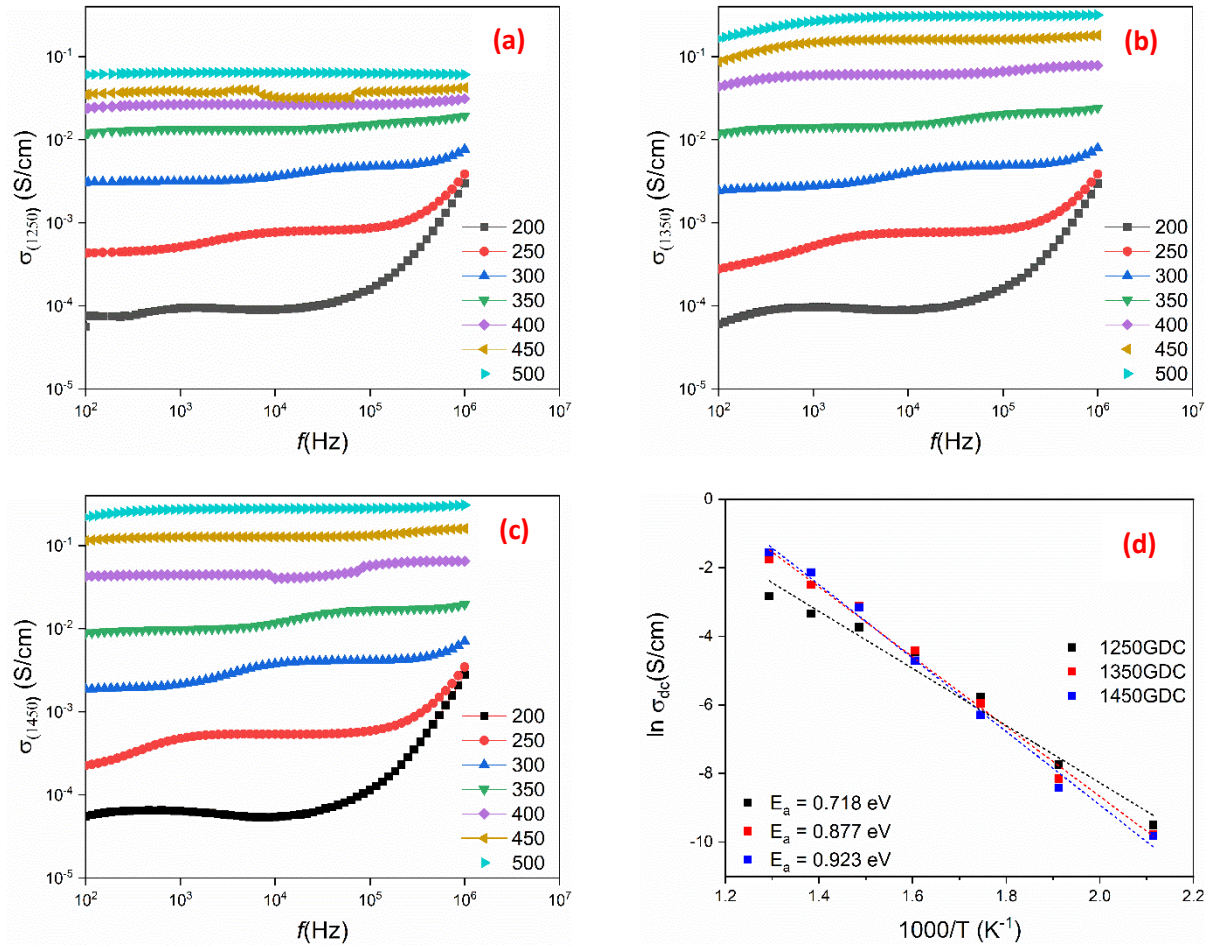


Fig 4.10 (a), (b), (c) AC conductivity behaviour with frequency of sintered sample in temperature range 200-500° C, (d) Variation of $\ln(\sigma)$ with $1000/T$ for activation energy calculations.

Fig 4.10 (a), (b), (c) represents the behaviour of AC conductivity with frequency at different sintering temperature (1250, 1350 and 1450° C) of the samples. Conductivity of the samples is calculated using dielectric data via following relation

$$\sigma_{(ac)}(\omega) = \epsilon_0 \omega \epsilon'' = \omega \epsilon' \tan \delta$$

where, ϵ'' , ϵ' , ϵ_0 and $\tan \delta$ are the imaginary permittivity, real permittivity, permittivity of free space and loss tangent respectively. The AC conductivity behaviour with frequency and temperature of all the sample is similar. It is observed that the conductivity is linear upto $\sim 10^5$ Hz (plateau region), which is attributed to the random ion diffusion in the present samples. This can be explained in context to mobile ion diffusion and long range order of transportation with

applied electric field. Above $\sim 10^6$ Hz, there is an increase in the AC conductivity. This can be due to the fact that heat is sufficient to excite more electrons, which leads to more hopping and thus σ_{ac} increases. The σ_{ac} for the sample sintered at 1250° C, 1350° C, 1450° C found to be 6.04×10^{-2} S/cm, 2.88×10^{-1} S/cm and 3.04×10^{-1} S/cm, respectively. With increase in the temperature the mobility of the mobile ion increases which leads to increases in the overall conductivity of the ceramic materials. Fig 4.10 (d) show the temperature dependent conductivity of the samples in the temperature range of 200-500° C via variation of $\ln \sigma_{dc}$ as a function of temperature. It is observed that for sintering temperature 1350° C and 1450° C the plot is almost linear up to a critical temperature $\theta_D/2$ (θ_D = Debye temperature) after which there is the change in the linearity of the plots, which indicate the temperature dependent activation energy of conduction. This conductivity behaviour is governed by Jonscher's universal power law i.e.

$$\sigma_{ac} = \sigma_{dc} + A\omega^n$$

where, σ_{dc} is the dc conductivity, σ_{ac} is the total conductivity, A is a constant that depends upon the temperature dependent, the angular frequency is represented by ω and n lies between 0 and 1 which depends on temperature and frequency exponentially. Arrhenius plot between σ_{dc} and $1000/T$ was plotted and is used to calculate the activation energy (E_a) of conduction:

$$\sigma_{dc} = \sigma_0 \exp(-E_a/K_B T)$$

where, σ_0 is pre-exponential factor, E_a is the activation energy and K_B is Boltzmann's constant [10]. It is found that as the conductivity increases the activation energy also increase, which is the reverse of the ideal trend [11-15]. The increase in the activation energy of the conduction process may occur when there is a reduction in concentration of the available charge carriers or when the mobility of the charge carriers declines due to the crystalline structure change or when both process occurs at the same time. These effects may reduce the agility of the anionic vacancies, lead to an increase in the activation energy [16] of the samples.

4.8 CELL TEST

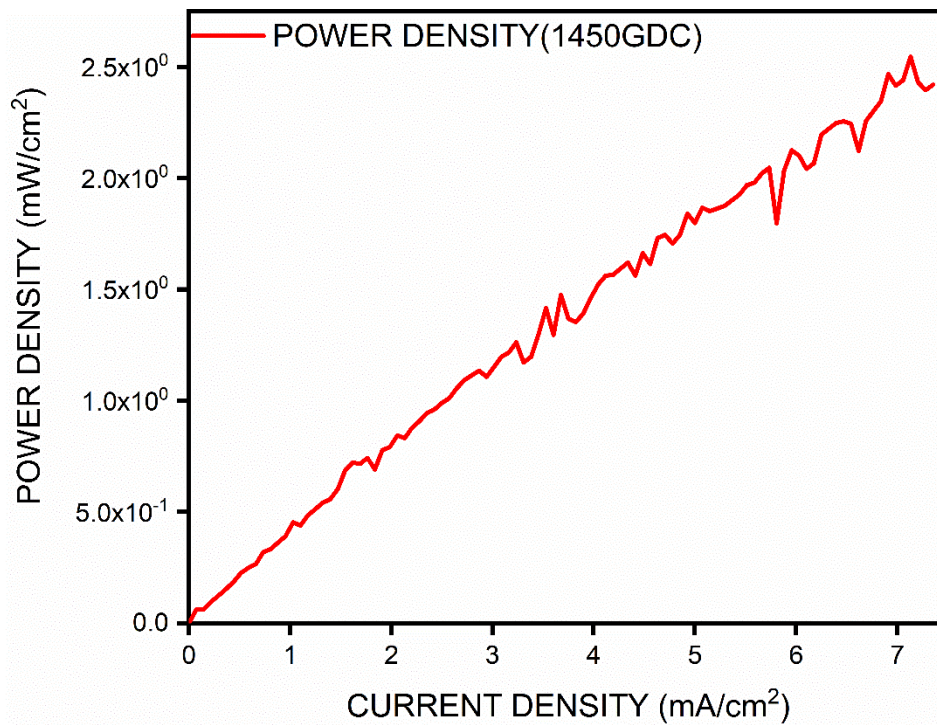


FIG 4.11 Power Density measurement of pellet sintered at 1450° C

Fig 4.11 show the power density measurement of the sample sintered at 1450° C. Platinum paste was used as cathode and anode on both side of the GDC pellet of diameter approx. 27 mm. The temperature of the furnace was raised up to 600° C with a heating rate of 5° C/min. The flow rate of the hydrogen gas to anode was set to 0.5 ln/cm². The power density was of 2.5 mW/cm² was obtained which is comparatively low as reported in the literature [17]. It may be attributed to the (a) contribution of electron to the total ionic conductivity of the sample (b) the pellet may be not sufficiently dense to prevent the leakage current (c) there may be formation of crack during the sintering on the surface of the pellet. This work can be perused forward to increase the total power output of the GDC electrolyte.

REFERENCES

1. Aliye Arabacı, n, M.Faruk Oksuzomer, Preparation and characterization of 10mol% Gd doped CeO₂ (GDC) electrolyte for SOFC application, *Ceramics International*, 2012, 38, 6509-6515
2. J. Chandradass, Baekil Nam, Ki Hyeon Kim, Fine tuning of gadolinium doped ceria electrolyte nanoparticles via reverse microemulsion process, *Colloids and Surfaces* 348, 2009, 130-136.
3. Yen-Pei Fu, Microwave-induced combustion synthesis and ionic conductivity of Ce_{0.8}(Gd_{0.2x}Sm_x)O_{1.90} ceramics, *Ceramics International* 34, 2008, 2051–2057.
4. Grazia Accardo, Claudio Ferone, and Raffaele Cioffi, Influence of Lithium on the Sintering Behaviour and Electrical Properties of Ce_{0.8}Gd_{0.2}O_{1.9} for Intermediate-Temperature Solid Oxide Fuel Cells, *Energy Technology*, 4, 2016, 409 – 416
5. A. Venkata Subramanian, Synthesis and characterization of doped ceria and doped barium cerate composite electrolytes for intermediate temperature Solid oxide fuel cells, Thesis, 2011.
6. Jayant Kolte, A.S. Daryapurkar, Mohit Agarwal, D.D. Gulwade, P. Gopalan, Magnetoelectric properties of microwave sintered BiFeO₃ and Bi_{0.90}La_{0.10}Fe_{0.95}Mn_{0.05}O₃ nanoceramics, *Materials Chemistry and Physics*, 193, 2017, 253-259.
7. S. Kazlauskas, A. Kezionis, T. S alkus, A. F. Orliukas, Effect of sintering temperature on electrical properties of gadolinium-doped ceria ceramics, *J. Mater. Sci.*, 50, 2015, 3246–3251.
8. R. O. Fuentes, R. T. Baker, Synthesis and properties of Gadolinium-doped ceria solid solutions for IT-SOFC electrolytes, *International. Journal of Hydrogen Energy*, 33, 2008, 3480 –3484.
9. T. van Dijk, A. J. Burggraaf, Grain Boundary Effects 04 Ionic Conductivity in Ceramic Gd_xZr_{1-x}O_{2-(x-2)} solid solutions, *Physica Status Solidi*, 63, 1981, 229–240.
10. Savidh Khan, K. Singh, Effect of MgO on structural, thermal and conducting properties of V_{2-x}Mg_xO_{5-δ} (x=0.05–0.30) systems, *Ceramics International*, 45,2019, 695–701.
11. R. V. Mangalaraja, S. Ananthakumar, M. Paulraj, K. Uma, M. Lypez, C. P. Camurri, R. E. Avila, Electrical and thermal properties of 10 mol% Gd³⁺ doped ceria electrolytes

- synthesized through citrate combustion technique, *Processing and Application of Ceramics*, 3, 2009, 137–143.
12. C. Veranitisagul, A. Kaewvilai, W. Wattanathana, N. Koonsaeng, E. Traversa, A. Laobuthee, Electrolyte material for solid oxide fuel cell derived from metal complexes; Gadolinia Doped Ceria, *Ceramic International*, 2012, 38, 2403–2409.
 13. X. Li, Z. Feng, J. Lu, F. Wang, M. Xue, G. Shao, Synthesis and electrical properties of $Ce_{1-x}Gd_xO_{2-x/2}$ ($x = 0.05–0.3$) solid solutions prepared by a citrate–nitrate combustion method, *Ceramic. International*, 38, 2012, 3203–3207
 14. K. Huang, M. Feng, J. B. Goodenough, Synthesis and Electrical Properties of Dense $Ce_{0.9}Gd_{0.1}O_{1.95}$ Ceramics, *Journal of the American Ceramic Society*. 81, 1998, 357–362.
 15. A. Sin, Y. Dubitsky, A. Zaopo, A. S. Arico, L. Gullo, D. La Rosa, S. Siracusano, V. Antonucci, C. Oliva, O. Ballabio, Preparation and sintering of $Ce_{1-x}Gd_xO_{2-x/2}$ nano powders and their electrochemical and EPR characterization, *Solid State Ionics* 175, 2004, 361–366.
 16. Licurgo Borges Winck, Jorge Luiz de Almeida Ferreira, Jesus Mauricio Gonzalez Martinez, Jose Alexander Araujo, Ana Candida Martins Rodrigues, Cosme Roberto Moreira da Silva, Synthesis, sintering and characterization of ceria-based solid electrolytes co-doped with Samaria and gadolinium using the Pechini method, *Ceramics International*, 43, 2017, 16408-16415.
 17. Leeba Khan, Pankaj K. Tiwari, Suddhasatwa Basu, Development of melt infiltrated gadolinium doped ceria-carbonate composite electrolytes for intermediate temperature solid oxide fuel cells, *Electrochimica Acta* 294, 2019, 1-10.

SUMMARY

Gadolinium doped ceria ($\text{Gd}_{0.1}\text{Ce}_{0.9}\text{O}_2$) was prepared via sol-gel process. FTIR analysis shows that at calcination temperature of 600°C most of the organic materials are removed from the samples. The prepared powder was calcined at 200°C , 400°C , 600°C . Single phase cubic fluorite structure with no secondary phase was obtained for as-prepared powder without calcination and its crystallinity increase as the sintering temperature increases. The prepared and calcined powder was characterized with XRD, FTIR, SEM, TGA/DTA, I-V and impedance analysis techniques. As confirmed by SEM analysis the pellets sintering at 1450°C yield a relatively highly density, thus makes it a most effectual way to produces highly dense ceramics. Also, high temperature sintering results in a significantly high ionic conductivity of $3.04 \times 10^{-1}\text{ S/m}$ at 600°C in air atmosphere. The mechanism proposed to explain the relatively high ionic conductivity can be the dopant ion mobility, small grain size, and highly dense packing of the grains. Complex impedance spectra with well defined, regular and symmetrical semi-circles, was observed in accordance to bricklayer theoretical model. It is in perfect co-relation to explain the microstructure and electrical properties of the samples. Impedance spectroscopy shows that as the temperature increase the two semi-circles start merging together and thus bulk and grain boundary conductivity can not be completely distinguished and grain boundary arc also start disappearing.

FUTURE SCOPE

- To develop better ionic conductors, it is important to lessen the activation energy, mobile ion concentration, and ionic jump distance within the lattice.
- With the dawn of efficient production techniques, micro SOFC is also evolving as an active research area to meet the requirements of portable applications.
- Despite the optimization of the electrolyte property for IT-SOFC, it is also important to design new anode and cathode materials with better performance (catalytic) to produce an efficient energy system in order to satisfy the new and increasing energy demands.
- The manufacturing cost and the operating temperature of solid oxide fuel cell is essential factor that is to be reduced.